ON MECHANISMS OF GLARE

J. J. VOS

INSTITUTE FOR PERCEPTION RVO-TNO
NATIONAL DEFENCE RESEARCH ORGANIZATION TNO
SOESTERBERG
THE NETHERLANDS

ON MECHANISMS OF GLARE

ON MECHANISMS OF GLARE

J. J. VOS

INSTITUTE FOR PERCEPTION RVO-TNO
NATIONAL DEFENCE RESEARCH ORGANIZATION TNO
SOESTERBERG
THE NETHERLANDS

FOREWORD

One of the main problems of the illuminating engineer is to avoid effects of glare. He continually meets with those effects and they are a handicap in his efforts to attain good lighting conditions. Eminent investigators as Holladay, Stiles, le Grand and Fry have provided him with quantitative data to evaluate the effect of glare in advance and this means a marked progress compared with the method of trial and error. Unsatisfactory, however, is our rather deficient knowledge of the origin of glare. There is a sharp controversy, whether glare is due only to entoptic straylight — so that it should be considered as a pure contrast phenomenon — or that there is some nervous "actio in distans" along the retina as well. A study of the literature and own experiments — described in earlier reports — taught, that elucidation of this controversy could not be expected from relatively simple experiments on glare evaluation in daily-life lighting conditions. More refined methods of investigations had to be used. During his research, Vos gradually got more and more convinced that possible nervous processes play a minor role at most. Once having come so far, he decided to advocate, with his full weight, a pure straylight concept of glare. In this thesis he accounts for his concept.

The first chapter, he walks the beaten road, while checking again the proportionality between glare intensity and its masking effect. This has always been a strong argument in favor of a straylight explanation. By his particular choice of perceptual conditions, however, he was able to add new data, which put him on the track of a notable fundus component in entoptic scatter. From then on he concentrated on an experimental and theoretical approach, which might give more quantitative and detailed information about the contribution of cornea, lens and fundus to the entoptic masking veil. High lights in this subsequent study are the experimental evidence for roughly equal parts, played by each of these three main scatter sources and the replacement of the too simple "diffusing sphere" model of the fundus by a more refined — though rather speculative — multi-layer concept.

Already in the first part, a highly suggestive proposal is made as to a difference in masking effect of fundus straylight at scotopic and

photopic conditions. The difference between the directional sensitivity patterns of rods and cones in thought responsible for it. In this respect attention must be drawn to the serious protanomaly of the author, who was the only subject in most experiments. For normal observers, vision at large wavelength is always photopic. This might give red the merit of being less glaring at low brightness levels. Dominance of rod vision in the author's eye in the red too, seems to have masked this effect and a further experimental check is certainly necessary.

In all experiments, the author made use of typically laboratory methods in conditions which were rather remote from those in practical situations. Thus, the lighting engineer will not find numerical data for direct application in practice. Basic research often asks for an experimental set-up, quite different from what the practitioner would consider opportune. But in our opinion, we have to go along this way to make real progress in the understanding of glare phenomena and in their evaluation in daily life situations as well. The present study contains a lot of starting points for further, also applied, scientific research. The influence of age, of pigmentation, of visual defects and eye diseases might be studied more to the point in the light of this concept. We can only hope that Vos himself, who obtained with this study his Ph.D., will find the opportunity to supply to his thesis such practical additions.

Maarten A. Bouman.

Erratum:

The expression between brackets in Formule 7.6(14) (page 65) should be read:

$$\left[\frac{H}{2R}\ \frac{1+g}{\vartheta^3} - \frac{g}{\vartheta^2} + \frac{1+g}{2\vartheta} + \frac{R}{2H\vartheta}(g-\vartheta/2)^2\right]$$

The main contribuants to entoptic scatter in the author's right eye.

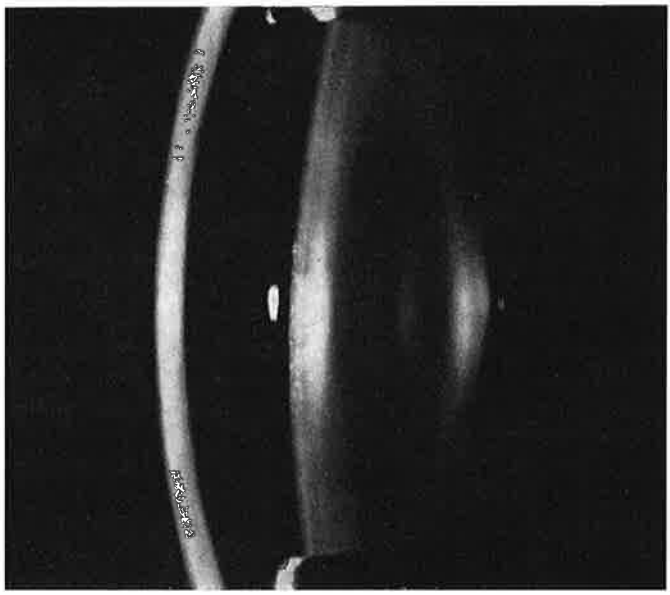

The cornea and crystalline lens, as they light up in slit lamp examination. The sharp light spot, just in front of the lens surface is the cornea reflex image of the slit.

(Own photograph)

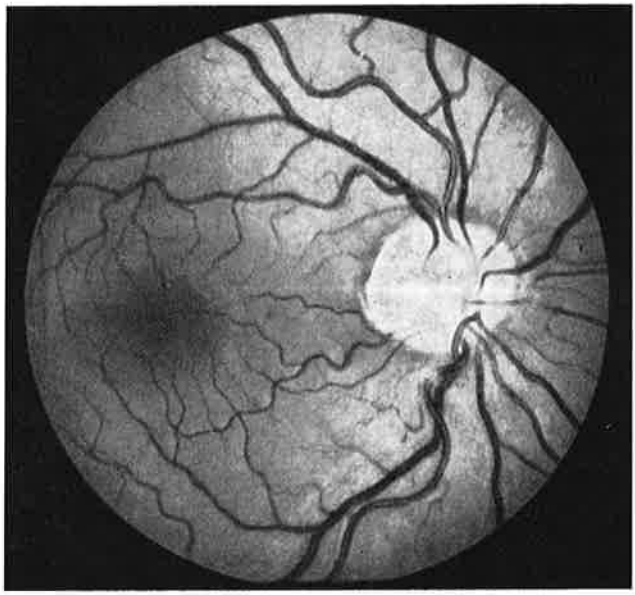

The fundus oculi, as it is seen in ophthalmoscopy.
(Photograph Royal Dutch Eye Hospital, Utrecht, with kind permission)

CHAPTER I

INTRODUCTION

1.1 The problem

When a strong light source enters the field of view, it appears as though a veil of light were thrown over the world outside. Close to the light source we are almost completely blinded, but further away too, visual performance is notably hampered. This experience, well known to participants in modern traffic — and who does not participate? — is usually called "glare". The importance in traffic in particular, has led to many practical studies, and we are well informed about its masking action, its unpleasantness and how to avoid it. Less complete, however, is our knowledge about the origin of glare. Two main currents can be discerned: that which seeks for an explanation in terms of entoptic straylight — this would directly explain the veiling appearance — and that which thinks in terms of a nervous inhibition. These descriptions both have their arguments pro and con, but many points are insufficiently stated to allow definitive conclusions. The aim of this thesis is to elucidate some of these controversies about the mechanism of glare.

From this it will be clear, that we take "glare" in a restricted way. So we will leave out of consideration the direct blinding effect of the glare source proper (a question of retinal over-exposure, associated with after-effects), and psychological aspects like discomfort and fatigue. In this thesis we will only study glare in the sense of:

"The hampering influence of a light source on visual functions, elsewhere in the field of view".

Exactly what, and how we will study, can only be told after a short survey of history.

1.2 Survey of history

The first communications about glare date from the beginning of the 19th century, and from the outset, the two trends: "straylight"

and "inhibition" stand out. Goethe (1810) devotes some pages to "subjective halo's" in his *Farbenlehre* and explains them in terms of a "conflict between mover and moved", like a stone (mover), thrown in the water (moved), causes a wreath of waves which spreads over the surface. A somewhat free translation in modern terms: in the nervous system of the retina, the stimulus of the bright light causes a disturbance, which, like waves on the water, spreads in all directions, gradually fading out. And with this view, Goethe can be regarded as the first in a long row of investigators, who think of glare as an essentially nervous process.

On the other hand, there is the second group, the first representative of which is Purkinje (1823), who emphatically ascribes the veiling appearance to scattering in the ocular media. Neither Goethe, nor Purkinje, did experiments to support their statements. However, by mentioning their names, we give them the recognition that they, first of all, have well observed and described these phenomena.

As a starting point of further scientific approach, we can best consider a paper of Helmholtz (1852). He clearly states that there are two possibilities: a nervous and a physical explanation; that scattering processes certainly occur, and that only further investigation will show what role nervous processes might play besides. It is not our purpose to follow closely the historical line; we will only mention the main arguments pro and con both concepts.

The main arguments in favor of a straylight explanation are as follows. First, entoptic scattering processes can objectively be demonstrated (with the slitlamp technique e.g., see frontispiece), and experiments by Boynton and co-workers (1954) on excised eyes have made it not improbable, that there is enough straylight to explain the experimentally found reduction in visual performance in terms of a masking veil. Second, there is a strong parallelism between the masking influence of a glare source and of an ectoptic (in contradistinction to entoptic) haze (Holladay 1926/27, Stiles and Crawford 1935/37, Le Grand 1937, Boynton e.a. 1954 and other investigators). And finally: the masking influence seems to be almost independent of the position of the glare source in the field of view (in the case, of course, that the angle of glare does not change). Neither the blind spot, nor the fovea, seems to take an exceptional position in this (Stiles and Crawford 1937). This might easily be understood from the straylight point of view, but difficultly, when we think in terms of neural mechanisms.

Objections against these arguments are, that most experiments cannot completely stand the test of criticism: steady fixation and artificial pupils are not always used (so that the experimental equivalence between the glare and the ectoptic veil experiments was insufficient), and moreover the parallelism is not always as nice as suggested, like Le Grand (1937) demonstrated. Finally, theoretical approaches never gave a satisfactory quantitative, or even qualitative description of glare phenomena (Stiles 1930, Fry 1954).

On the other hand, there are many arguments in favor of a nervous interaction as a cause of glare. The most frequently cited author is Schouten (1934/39), whose main argument is the marked difference between the dynamic behavior of glare and of an ectoptic veil. His arguments are weakened, however, since his results could not be reproduced by others as Fry and Alpern (1953[1]). Besides, he has not sufficiently explored the straylight explanatory facilities, and many of his arguments might be reversed as well. Next, one usually finds reference to the electrophysiological work of Kuffler (1953), Barlow (1953) and others, who found inhibitive areas around the stimulated point. The trouble with these experiments is — like Kuffler, for instance, admits — that it is difficult to relate the findings to psychophysical data. Besides there is the — strongly questioned — work of Motokawa (1950), who denies inhibition and speaks of facilitation.

Of more weight in my opinion, is the influence of the environmental illumination on photometric accuracy. That strong illumination of the surroundings of a bipartite photometric field lowers the matching accuracy, might be explained by entoptic straylight as well. But the accuracy decreases again, when the environment becomes darker than the photometric field (Cobb and Geissler 1913). In this way one would be inclined to think of a nervous mechanism, which passes through a minimum at uniform brightness. Strangely enough, this argument is seldom put forward in modern literature about glare and seems to be more or less forgotten.

With this example, we left the field of glare proper, and indeed, when we consider adjacent areas of visual science, we note many phenomena, which can hardly be explained in terms other than neural interaction. One can find neural summation (of below-threshold stimuli: Van den Brink and Bouman 1954, Van den Brink 1957) as well as neural inhibition — and we think of contrast phenomena (color, brightness and border) and the closely associated Mach phenomena (Mach 1865). Though part of these contrast phenomena is

not purely spatial presumably, like Fiorentini and Ercoles (1957) demonstrated, it seems to be beyond doubt that neural inhibition between neighboring elements plays a role. The seat of this inhibition may be retinal, but very central processes might play a role as well. In this connection it is interesting to regard one example, taken from Benary (1924) and reproduced below (Fig. 1.2.1).

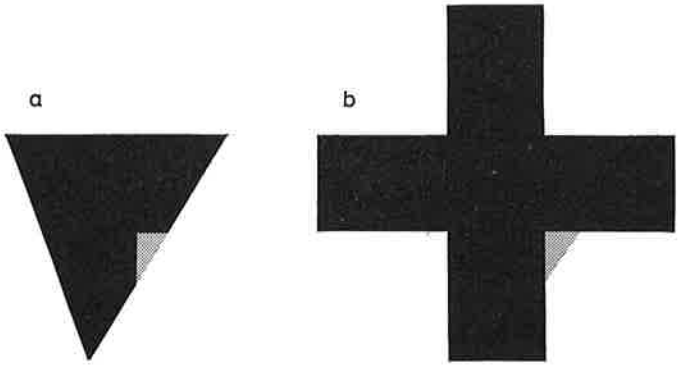

Fig. 1.2.1. The gray triangle in *b* has a darker appearance, though it has more dark in its surroundings. An example of a non-physical, probably very central interaction (Benary 1924).

One easily verifies, that *a* is identical with the central part of *b* and that *b* only contains more extended black parts. Now it is well known, that a gray disc on a white background has a darker appearance than the same disc on a black background (brightness contrast), and so we should expect here — if any effect at all — that the gray triangle in *a* has the darkest appearance. Actually we see the reverse, because of the different weight of the place of the triangles in both figures: in *a* it disturbs the "Gestalt", in *b* it does not. To all physical determinants, a psychical factor is added, and that is what tips the scale here.

With this example we have wandered far from our original subject of interest, the study of glare. The brightness contrasts in this figure are so small that no one indeed would even think of glare. Its instructiveness lies in its exaggeration. By exceeding the area of our subject proper, we come into a position of prospect, which allows us to survey this area and to give a further specification of its boundaries. We have discovered, that there certainly is a physical component in glare, even though its qualitative and quantitative behavior is far

from elucidated. The existence of a peripheral nervous component seems to be less certain. The most pregnant demonstrations of non-physical effects point more to central, psychical phenomena. At the same time we learned that these psychical phenomena essentially do not belong to our subject, so that we have to get rid of them in studying glare proper.

Now our provisional reconnaissance has taught us, that non-physical factors appear exactly, where the relatively complex criterion of "brightness impression" (matching, judgement) is used as a measure of interaction. As long as we restrict ourselves to simple experiments, like threshold determinations, these factors seem to be of minor importance. In this connection we refer to Ives' finding (1912), that in heterochromatic photometry, the results are only independent of the surroundings, when we apply flicker photometry or the "step by step" method. The direct simultaneous matching, however, is clearly influenced by the environmental illumination. Again: as the experiments grow more and more intricate, peripheral mechanisms become inadequate to explain our perception and higher centra will be involved.

1.3 Our program

Our considerations mentioned above lead us to the following further specification of our aims:

We will study the mechanisms of glare. Our concept of it will be restricted to the peripheral, physical and neural, masking influence of the glare source on its surroundings. Central, psychical effects will be regarded as artefacts, which should be avoided and might be avoided by a suitable experimental technique: by the use of simple criteria (threshold determination) and by the elimination of attention as a determining factor (flashing objects).

Our first goal will be the verification of the absence or presence of a nervous component by studying, in a conventional way, the parallelism between the glare veil and an ectoptic luminous veil (Chapters II and III). Anticipating the results, we mention that the presence of a nervous component could not be ascertained. This allowed us to pay full attention in the next chapters to the scattering processes in the ocular media, first experimentally (Chapters IV, V, and VI), next theoretically (Chapter VII). Chapter VIII finally, is used to construct a picture, which best accounts for all theoretical and experimental data.

Restriction

The results of psychophysical experiments, and of glare experiments in particular, may differ from subject to subject. In most of the experiments described, the author has acted as subject. The following data might be relevant as to their interpretation. During the experiments he was round about thirty years. He has a fair complexion, with light brown eyes. His color vision is defective (strongly protanomalous according the H.R.R. classification).

CHAPTER II

THE EQUIVALENT VEIL

2.1 Purpose and method

The best way to verify the existence of a nervous component in glare phenomena is to approach the problems as though the disturbance of the visual performance were only due to straylight. Eventual deviations from the relatively simple physical laws then point to physiological or psychological influences. The method of the "equivalent veil" walks this way. Introduced by Cobb (1911), refined by Holladay (1926) and Stiles (1929) among others, it comes to this. The behavior of some, mostly static, visual function (visual acuity, or contrast threshold e.g.) is investigated *a.* under conditions of glare, and *b.* when the visual field is masked by an ectoptic luminous veil. In the literature the term "background" is frequently used, which insufficiently accounts for the fact that the background is not obscured by the test object. The expression "veil" better describes the masking situation. Both glare and ectoptic veil produce a rise of the threshold, a decrease in visual acuity — or whatever is taken as a test function. Let us consider the contrast threshold, to fix our mind. Let us further assume equivalence between the experimental glare and veil situations as far as possible: the experiments are performed at the same width of the pupil, with the same test object, which has the same place in the field of view and so on. In principle, the course of the brightness over the field of view should be the same too, but usually, the comparison field is chosen homogeneous for technical reasons. Le Grand (1937) has shown, that the lack of equivalence, introduced in this way, has no serious consequences, at least in foveal perception. Now, that veiling brightness (B), that causes the same rise in contrast threshold as a given glare source (the intensity of which is usually indicated in terms of the illumination E, produced in the plane of the pupil), is called the "equivalent veiling brightness" (B_{eq}). On the ground of the basic assumption (entoptic straylight only), we should

expect a strict proportionality between B_{eq} and E for one, otherwise unchanged glare situation. Or, introducing the

$$\text{blinding capacity } C = B_{eq} / E, \qquad (1)$$

the invariance of C against E is a check on the likeliness of this assumption. The next table gives a survey of the experimental conditions and the results of the main investigators, using the equivalent veil method.

Table 2.1.1

Results of the main investigators, using the equivalent veil method

Author	Criterion	Pupil	Presentation of the target	Range of E-values	Results
Cobb (1911)	Visus	Artificial	Steady	Factor 32	C increasing with E
Holladay (1927)	Just visible brightness	Natural	Steady	Factor 24	C increasing with E
Stiles (1929)	increment	Natural	Steady	Factor 20	No systematic deviations from C = constant

The results of all three investigators are not far from C = constant over E, but deviations cannot be denied. In view of our demands, formulated in § 1.3, these somewhat irregular results do not surprise. The criterion of "just visible" in a steady presentation is rather complex, because a steady target has a small intrinsic conspicuity (attention as a complicating factor), and pupillar contractions were only eliminated by Cobb. Besides, the range over which E was varied is relatively small in view of the logarithmic behavior of most visual functions. Therefore, we had some reason for an improved repetition of their measurements.

2.2 Experimental arrangement and procedure

The experiments were performed with the apparatus, represented in Fig. 2.2.1. Two light paths — one providing the imaging of the glare source, respectively the ectoptic veil, the other one imaging the test object — are mixed by M_1 and M_2 so as to give one field of

view V. The optics of both light paths are quite similar. We made use of it by giving the imaging of the field of view in the upper half (hatched beam), the imaging of the light source (tungsten ribbon lamp) in the lower one. Beam profiles and limitations are symbolically indicated as marginal silhouettes at various points.

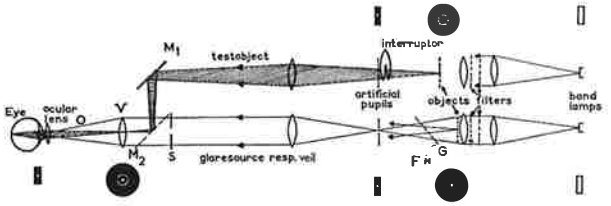

Fig. 2.2.1. The optical arrangement. A glare / veil beam and a test beam are mixed at M_2, to give the common field of view V in Maxwellian view. In the lower beam, the path of light coming from the light source is given, in the upper beam the focusing of the objects in the field of view (hatched). The marginal silhouettes indicate cross sections through the beams as they occurred in the experimental conditions of Chapter 2.

The main characteristics of this arrangement are:

a. In glare experiments a field stop with a small aperture (making the glare source) was interposed at "objects". In the veil experiments no diaphragm was used, so that a uniformly illuminated field of about 18° diameter was visible. With white light, the intensities were regulated with neutral filters in steps of a factor 10 and with the stabilized feed current for minor variations only, so that the color temperature did not notably change.

b. A beam limitation at the entrance of the eye was arranged by interposition of a diaphragm at the first image of the light source. These diaphragms, in turn, were imaged at the pupil of the eye. This imaged artificial pupil, mostly 1 mm in diameter, has the same effect as a real artificial pupil, but the advantage besides, that it gives no harmful straylight at its edge. Moreover we can easily interrupt now the test beam without intercepting the other light path.

c. The direction of fixation could be determined with the auxiliary lamp F, which inserts its light via the glass slide G.

d. A difficulty of lens-rich equipments like this one, is the amount of false light evoked by multiple reflexions and scattering by dust. Of course, this false light is only important for the glare beam. Thanks to the large depth of focus (small artificial pupil) we were able to cut off most straylight by interposition of a diaphragm, only somewhat larger than the glare source, at S, though no image proper is formed at this place. Straylight, evoked at M_2 or at V has no influence, as it is focused as well on the retina. Remains the ocular lens, which indeed has to be cleaned regularly and carefully. As a result, the straylight, due to the apparatus, amounted only some 5% at

most, of the equivalent veiling brightness at the corresponding angle of glare. This could be verified in photo-electric test experiments (compare Fig. 2.3.4).
e. The position of the eye with respect to the exit pupil of the apparatus was sufficiently fixed with a head rest, consisting of a chin rest, a nose clamp and temple supports. Its sufficiency could easily be controled at the higher glare intensities, when the shadow of the iris becomes visible, like it is projected from the cornea as a scatter center. This shadow can be centered round the glare source and excellently maintained so with the head rest.

Each two seconds, the interruptor made the object flash during an adjustable interval. In most experiments, the flash time was chosen 0.5 sec, which is short enough to suppress possible attempts for scanning and has the advantage that we can measure in a region, where the threshold of perception — which will be our criterion — is strongly dependent on the level of adaptation (Bouman 1950). Moreover, the experience has learned that the accuracy of the threshold determination increases — within certain limits — with increasing flash time. The threshold of perception was determined, by means of counters, as the 50 % chance value of a frequency of seeing curve.

The description above is kept in general terms, because the same apparatus will be used in other, later in this thesis described experiments too. We have to make some further specifications for our present goal. The glare source is presented centrally (thus: glare source = fixation light), the test object as a ring round about. This condition we will indicate as "foveal blinding, peripheral perception" throughout this thesis. The attending silhouettes of Fig. 2.2.1 represent this situation. We could chose this test condition, because both the sensitivity of the retina round the fovea and the blinding influence round the glare source are circularly symmetric (Stiles and Crawford 1937). By this choice of the experimental situation we attained, that the range of available glare intensities is large (peripheral vision); that the test object has a maximum extent for each angle of glare (which has a similar influence as a long time of presentation; see above); and that the observer is not inclined to loose his fixation, in order to search for the object (no preferential direction).

In these first experiments, no color filters were inserted in the glare / veil beam in order to avoid a needless limitation of the range of glare intensities available. That the test object was always monochromatic (λ = 525 nm) for the easiness of calibration, is a matter of minor importance: the threshold plays a connective role only in the equivalent veil method and disappears from the final results.

2.3 The linearity check

The actual procedure is demonstrated in Fig. 2.3.1 together with Fig. 2.3.2a. The first figure shows the dependency of the threshold for one test ring upon the glare intensity and on the veiling brightness respectively, brought together into one picture. The resemblance of both curves finds its expression in the relation between the equivalent veiling brightness and the glare intensity corresponding with the same threshold value. This graph is constructed in the following way. Take an experimental point (a) on the glare curve, determine the corresponding point on the veil curve (b), and relate their abscis values (Fig. 2.3.2a). In this way, the spread of the experimental points of the veil curve is obscured in the final result, so that the accuracy of the latter is some $\sqrt{2}$ times less than suggested by the picture.

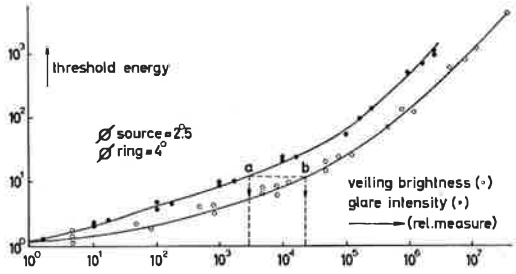

Fig. 2.3.1. The threshold of perception for one test ring as a function of the glare intensity (•) and of the ectoptic veil brightness (o) respectively. The mutual position of the two curves in a horizontal direction is arbitrary.

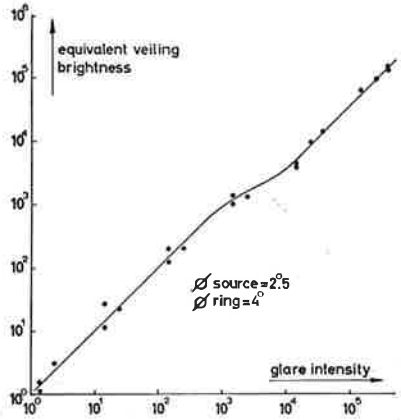

Fig. 2.3.2a. The relation between the equivalent veiling brightness and the glare intensity, as it is derived from the curves of Fig. 2.3.1. A straight line under 45° would mean a direct proportionality.

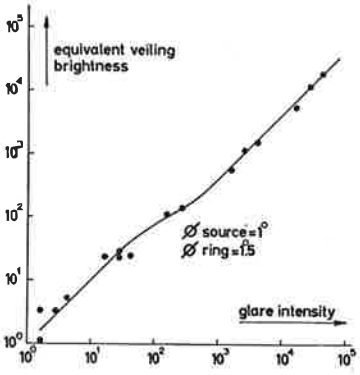
equivalent veiling brightness
Ø source=1°
Ø ring=1.5
glare intensity

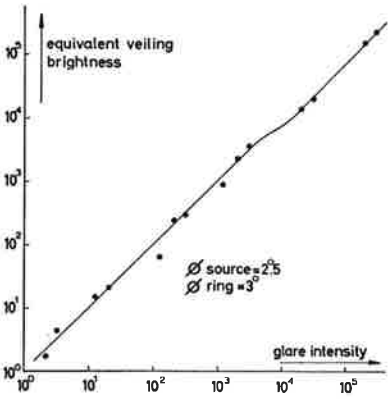
equivalent veiling brightness
Ø source=2.5°
Ø ring=3°
glare intensity

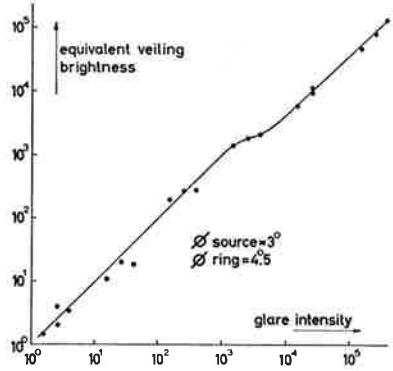
equivalent veiling brightness
Ø source=3°
Ø ring=4.5°
glare intensity

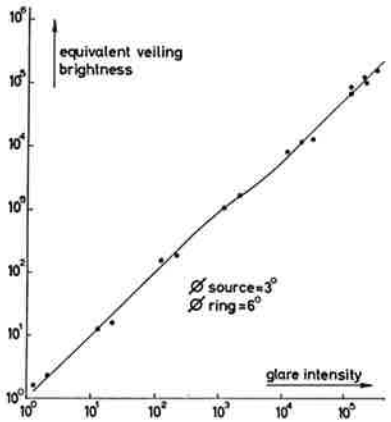
equivalent veiling brightness
Ø source=3°
Ø ring=6°
glare intensity

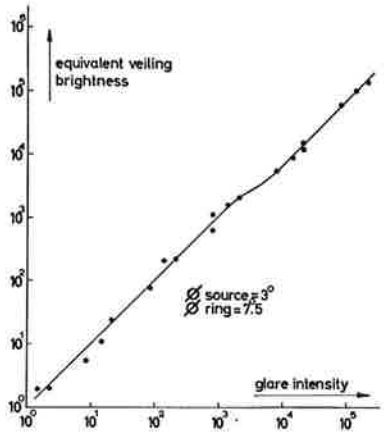
equivalent veiling brightness
Ø source=3°
Ø ring=7.5°
glare intensity

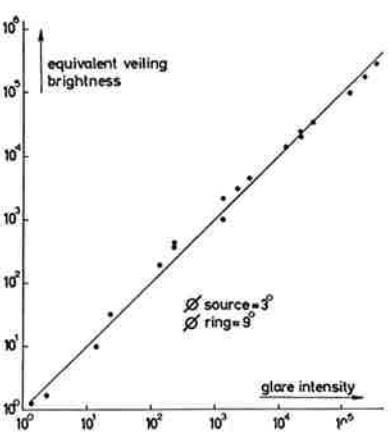
equivalent veiling brightness
Ø source=3°
Ø ring=9°
glare intensity

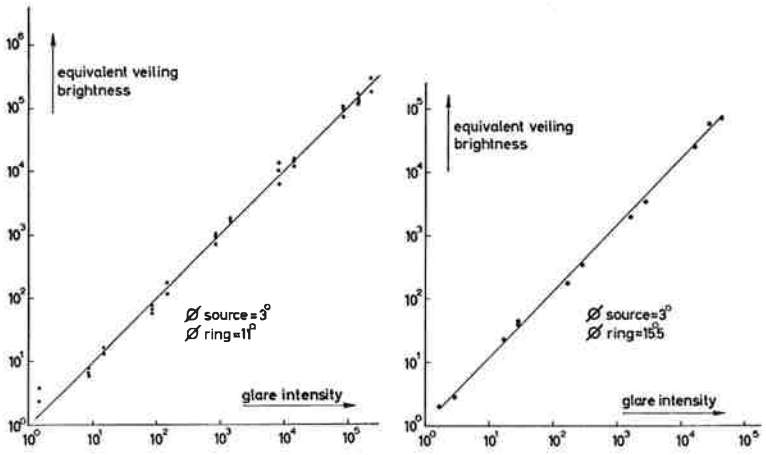

Fig. 2.3.2b. The same relation as in Fig. 2.3.2a, but for other angles of glare.

The other graphs of Fig. 2.3.2 give the same relation for the other investigated angles of glare (between glare angles 1^0 and 8^0). We note that the relation is strictly linear for the largest angles of glare — which appears from the course as straight lines under 45^0 in these graphs, which are logarithmic in either direction —, but that there are deviations from a linearity for the minor angles in the form of a bayonetlike inflexion. Like explained before (§ 2.1), these deviations from a linearity point to the presence of non-physical mechanisms.

The various graphs of Fig. 2.3.2 have been measured over a long time, and to avoid possible influences of a long term drift, their mutual positions have been determined afterwards in a separate session (Fig. 2.3.3) at one value of the glare intensity (at the vertical arrow).

To give the reader some hold as to the photometric level in an absolute sense, one glare intensity and one equivalent brightness are indicated in this figure. They are found by computation (from lamp calibration + Planck's law + conversion from Maxwellian to natural view + luminosity curve for the human eye) and experimentally checked with a calibrated lux meter. It draws our attention that the anomalous inflexions lie at about one level of the equivalent brightness, namely the middle mesopic value of 10^{-1} cd/m^2; definitely not at one level of the glare intensity E, anyhow.

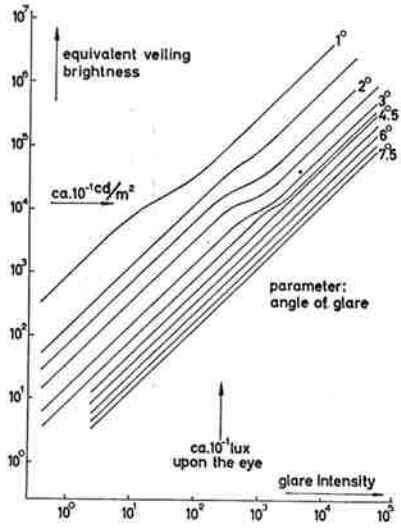

Fig. 2.3.3. The equivalent brightness as a function of the glare intensity for various glare angles. Composite graph, based as to the shape of the curves on the data of Fig. 2.3.2 and as to their mutual position on Fig. 2.3.4. Where no value of the glare angle is indicated, the middle between the adjacent values is meant. The arrows indicate approximately the absolute values of the light level.

Obviously, the course of the graphs cannot be explained in terms of entoptic straylight only. It is clear on the other hand, from the strictly linear relationship at large angles, that straylight is an important factor. It seems improbable, that the scatter mechanism changes, on physical grounds and because the inflexions lie at one level of B_{eq}, rather than E. A change in the receptor mechanism seems to be a more attractive assumption. We know such a shift, the Purkinje shift, which just occurs at the brightness level wanted. This shift, the transition from rod to cone vision, might give us the key to the explanation of the inflexion effect. We need to explain with it a divergence between the action of entoptic straylight and of normally incident ectoptic light on the retina. Now their only difference lies in the angle of incidence at the retina. Light from an ectoptic light source enters the eye via the pupil and has an about perpendicular incidence. Straylight can have any angle of incidence from perpendicular (cornea scattering) to striking (fundus scattering). Involuntary, our thoughts go into the direction of the Stiles-Crawford effect, which describes the directional sensitivity of the retina, and, just wanted behavior,

which comes into play at photopic levels only! We are strengthened in this concept by a "bizarre phenomenon", described by Le Grand in his thesis (1937), which has much in common with our inflexion effect. He found a rapid increase in brightness of the glare veil during the first stage of dark adaptation, especially for small angles of glare. The effect had the same order of magnitude as our jump round the inflexion. Le Grand too, looked for an explanation in the direction of the then recently discovered Stiles-Crawford effect.

We will not further elaborate this view for the moment and delay it to a more integral study of straylight mechanisms in the 7th and 8th chapter. Suffice it for the moment to state, that the directional sensitivity of the retinal cones can actually be thought to form a suppressive mechanism for non-perpendicularly incident straylight, in particular therefore for straylight originating from the fundus oculi. It might explain the jump if we assume, that the fundus contributes the major part to the entoptic veil for small angles of glare. From the course of the successive graphs of Fig. 2.3.2 we measure the following values of the jump factor: 3.0, 1.8, 4.2, 4.2, 2.6, 1.8, 1.0, 1.0, and 1.0 again respectively. These figures suggest an average jump over some factor 3 for the smaller angles of glare. Assuming a complete suppression of the fundus component in cone vision — an extreme assumption — we derive:

$$\frac{\text{entoptic straylight (without fundus comp.)}}{\text{entoptic straylight (including fundus comp.)}} = \frac{1 - \text{fundus comp.}}{1} = \frac{1}{3}$$

so that the fundus would furnish some 2/3 of the entoptic straylight at least at these angles — against an insignificant fraction at the larger angles investigated.

We indicated above, that the mutual position of the various curves of Fig. 2.3.3 was determined in a separate session. In these experiments, the equivalent veiling brightness was determined as a function of the angle of glare for one value of the glare intensity (10^{-1} lux at the pupil) and with a glare source which was small compared with the angles of glare concerned (ø glare source $\approx 11'$).

This relation itself is presented in Fig. 2.3.4, together with the photo-electrically determined amount of straylight from the apparatus (compare § 2.2d).

The glare curve is described best by

$$C = \frac{B_{eq}}{E} = \frac{29}{\vartheta^{2.8}} \qquad (1)$$

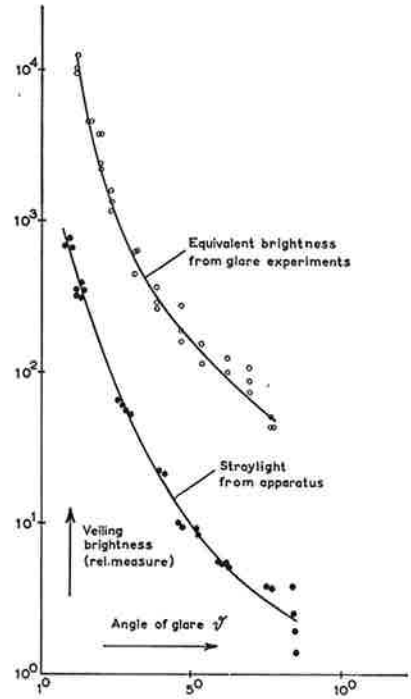

Fig. 2.3.4. The course of the equivalent veiling brightness with the angle of glare. For comparison, the photo-electrically determined amount of straylight from the apparatus is plotted too.

when we pass to absolute values. In Table 2.3.5 we compare this behavior with results found by other observers. As units we used the degree (ϑ), the cd/m^2 (B) and the lux (E), while C = B/E has the sr^{-1} as unit.

In the second row we added an uncertainty margin, which roughly indicates what is the minimum value of ϑ, which can be thought reliable in the sense of: large compared with both the size of the test object and of the glare source. The last row shows that our experiments diverge from the other investigations by that the test object was moved over the field of view, and not the glare source. What is the better way depends upon one's goal: for practical problems of illuminating engineering the situation of a changing eccentricity of the glare source should be preferred, for theoretical investigations a fixed glare situation seems to be required. In this connection we

Table 2.3.5

The relation $C = B_{eq}/E = C(\vartheta)$ as it is found in this and other investigations

Investigator	ϑ-domain	E-domain	Relation	Conditions
Holladay (1926)	$2.5° < \theta < 25°$ ± 7°	E = 1 lux Natural pupil	$C = \frac{9.3}{\theta^2}$	Glare source moved
Stiles (1929)	$1° < \theta < 10°$ ± 5°	E = 0.5 lux Natural pupil	$C = \frac{4.16}{\theta^{1.5}}$	Glare source moved
Stiles and Crawford (1937)	$1° < \theta < 102°$ ± 4°	E = 6 10^{-3} and 0.2 lux Natural pupil	$C = \frac{11.5}{\theta^{2.1}}$	Glare source moved
Le Grand (1937)	$1° < \theta < 30°$ ± 2°	$0.1 < E < 10$ lux Artificial pupil	$C = 13\,\theta^{-3} + 11\,\theta^{-1.5} + 4.10^{-3}\cos^4\theta$	Glare source moved
Fry and Alpern (1953[2])	$0.75° < \theta < 4.5°$ ± 2°	$5\,10^{-2} < E < 10^3$ lux Artificial pupil	$C = \frac{22.4}{\theta^{2.5}}$	Glare source moved
Vos (1963)	$1° < \theta < 8°$ ± 40′	$E = 10^{-1}$ lux Artificial pupil	$C = \frac{29}{\theta^{2.8}}$	Test object moved

should like to make the more general remark, that investigations on glare for the theory and for the practice can best be kept completely apart (Vos and Bouman 1959). The former require: an artificial pupil, a steady fixation and a steady glare source, the latter just the contrary. That there has been so little advance in our understanding of glare phenomena since Helmholtz (§ 1.2) is largely due to the fact that most studies halt between two opinions: to give results for the practice of lighting, and to furnish a contribution to the theory of glare.

Other investigators have never found a similar inflexion effect. This may be caused by the fact that this effect is connected to the transition from rod to cone vision. In experiments where the glare source is varied in place, the test object is usually detected with the fovea. Here no transition from rod to cone vision, no Purkinje shift occurs.

2.4 The dependency on wavelength

It is interesting to know the influence of the wavelength of the glare light on the blinding capacity from the practical as well as from the theoretical point of view. Therefore, we determined its course over the visible part of the spectrum. Interference filters were placed at "filters" (Fig. 2.2.1) in the glare / veil and in the test light path, always of equal wavelength transmission for both beams. At the ends of the visible spectrum, it was difficult to get enough brightness to produce a distinct rise in threshold. In the central region of the spectrum we had no difficulty of course.

The first experiments revealed, that there was no notable dependence on the wavelength for large angles of glare (Fig. 2.4.1b), but that there was a strong dip in the green region for small angles Fig. 2.4.1a). This proved to be an artefact, an interesting artefact though. All measurements were done at the highest brightness levels we could reach, and not at one constant level. The green masurements were done at a much higher level therefore, than the red and blue measurements and the dip in the green region could be tributed to the brightness jump, mentioned in the former section. Remeasurement at lower levels confirmed that the dip gradually filled up (arrow), so that finally the relation became almost horizontal for these angles too.

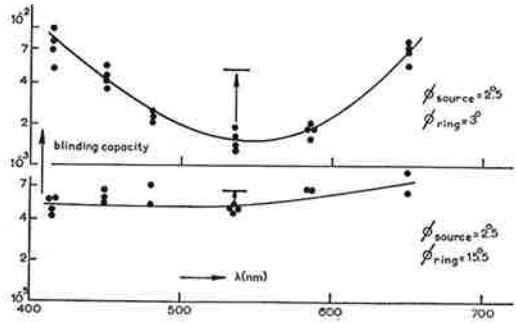

Fig. 2.4.1. The dependency on the wavelength of the glare light for a small and a large angle of glare. The experimental points are measured at the maximum available glare intensity for each wavelength. Consequently, the glare intensity was much higher in the green region than at the ends of the visible spectrum. Reduction of the glare intensity in the green made fill up the depression in the indicated way.

This independence of the wavelength of the glare light is best demonstrated, when we plot the blinding capacity for red against that

for blue under the same conditions (Fig. 2.4.2). The various experimental points only differ, because they are determined for rings of different diameters ($\sim \vartheta$). The deviations from equality cannot be thought to be significant.

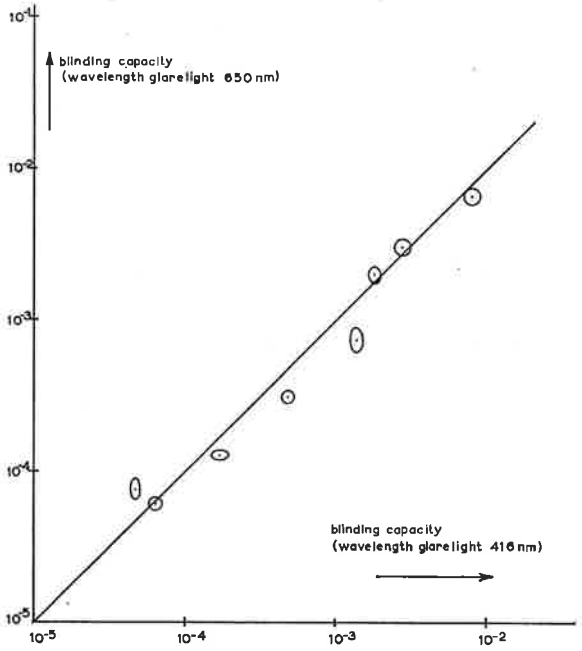

Fig. 2.4.2. The relation between the blinding capacity of a red and a blue glare source in the same experimental conditions.

So, the wavelength experiments lead to two conclusions:

a. The dependence of glare on the wavelength of the glare light is negligibly small.
b. The jump effect, found in the former section, was unexpectedly confirmed.

We might ask, why the dip in the green part of the spectrum does not extend to the red end, since red is said to stimulate cones only. Now there are indications, that this is not true for the author, who happens to be strongly protanomalous. Wald (1945) found that at 650 nm, the rods were only 2 to 3 times more sensitive than the rods at the same place, 8^0 above the fovea, and for a one degree field of view. Flamant and Stiles (1948) came — along another way — to

much the same value at 5^0 beside the fovea, now for 640 nm. Now the author's cone sensitivity is reduced by some factor 6 at the red end of the visible spectrum, so that there seems to be much reason to assume, that his parafoveal vision in the dark adapted state is rod vision up to far in the red.

Finally, we compare our results with those of other authors. Most of them worked with white light or only touched the problem of color dependency. Le Grand (1937) found, that red dominates for small angles of glare ($C_{red} \approx 1.3\ C_{white}$ for 1^0), but that blue is predominant at large angles ($C_{blue} \approx 1.4\ C_{white}$ beyond 7^0).

The origin of the divergence from our results is not clear and can not only be attributed to the higher accuracy (astonishing high even!), attained by Le Grand. Perhaps, the difference in the experimental conditions (Table 2.3.5) plays a role. Of other authors, only Ivanoff (1947) found a strong wavelength dependency, but his results cannot be compared with the equivalent brightness results (he used quite another way of quantification), and besides, his glare intensities varied over the spectrum, so that the jump effect might play a role, like it played a role in our experiments.

2.5 Conclusions

The experimental results, described in the preceding sections, lead to the following preliminary conclusions:

a. The presence of inhibitive neural effects could not be demonstrated.

b. The jumps in the blinding capacity round the mesopic zone, point to an unexpectedly large share of fundus straylight in glare — at least for small angles of glare.

c. The influence of the wavelength of the glare light seems to be small, if present at all.

CHAPTER III

CONTINUED SEARCH FOR RETINAL INTERACTION

3.1 Purpose and method

There are three reasons to continue our hunt for retinal interactions, in spite of the negative result of the foregoing chapter. The first reason is, that Bouman has found some indications for the presence of an inhibitive mechanism in slightly different circumstances. Second, the method he introduced, might allow conclusions besides the bare existence of neural effects and tell us something about the underlying mechanism. And finally, our experiments of the former chapter have all been performed with a foveally presented glare source and this very situation might be little apt to demonstrate neural effects.

The behavior of the absolute and the contrast threshold on the diameter or length of the target and on the time of presentation has been subject of extensive investigations by Bouman and Van der Velden. A survey of these investigations and their theoretical background has recently been published by Bouman (1960[1,2]). It is not necessary to go into details about this theoretical background and the interpretation of these experiments now. We only need for the moment, that the dependency of the threshold upon each of these parameters gives us an insight in the neural mechanisms in the retina. The change in this dependency with the level of adaptation informs us about the change in these neural mechanisms, that is: in the nervous component in adaptation.

Now we can also investigate this dependency in the presence of a glare source and follow it as a function of the glare intensity. Should this behavior go completely parallel with the course as a function of the veiling luminance ("background"), then we could fully explain the action of the glare source in terms of entoptic straylight. However, a systematic divergence between both relations would point to some other process which — and that is the specific advantage of this

approach — might be interpreted in terms of a quite definite process of nervous interaction in glare.

Bouman (1953) actually performed some preliminary measurements on the influence of the length of a test bar respectively under conditions of glare and background. They pointed to a difference between glare and background in their influence on the neural mechanism. These experiments were too few, however, and too fragmentary, to allow a definitive conclusion. The experiments, described below, are meant as a repetition, extension and refinement of these earlier experiments.

3.2 Procedure and results

The experimental arrangement was essentially the same as described in § 2.2. In the present experiments we choose the following conditions. The glare source was ring shaped, concentrically around the point of fixation. The test object was a part of a ring, just concentrically around the glare source (Fig. 3.2.1). The sector of the ring in use, could be varied between 360° (full circle) and 60° by superposition of the ring diaphragm and a sector diaphragm (Fig. 3.2.2a). Below 60° a hole diaphragm (b) was used, for technical reasons, in stead of the sector. For the smallest target (2°), the hole alone determined the size (c). To avoid misunderstandings, we will indicate in the next the object size, not by its sector value, but by the angle under which it would be seen, when completely unfolded. This angle, the length of the circumference, ranged from 8′ up to 24°.

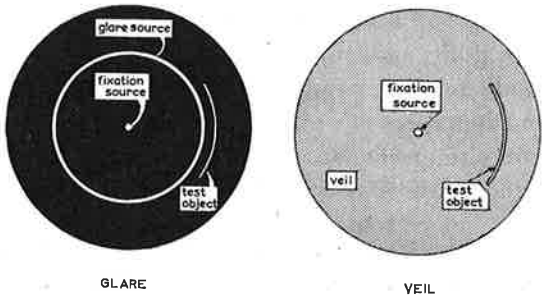

Fig. 3.2.1. The field of view in the glare and in the comparable veil situation. The diameter of the ring was 8°.

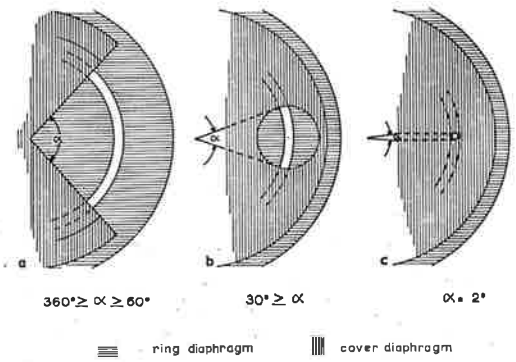

Fig. 3.2.2. The determination of the sector size with cover diaphragms.

By this particular choice of the form of the glare source and the object both, we attained that the angle of glare could be chosen small (see below), only a little bit larger than Ricco's area — about 10′ in diameter in this peripheral region (Van den Brink and Bouman 1954, Van den Brink 1957) — so that the experimental conditions were thought favorable for the appearance of neural effects. Further quantitative data are:

glare source	test object
diameter ring: 8°	diameter ring: somewhat larger
width ring: 12′	width ring: 14′
gap between them: 30′	
stationary exposition	flash time: 0.04 sec
color = color veil : white	color: green (λ = 525 nm)

The method of threshold determination was the same as formerly described. To prevent bias, we always measured only one object per session. Only after all measurement were finished, we could construct the threshold / length relation by plotting a "cross section" through the experimental data obtained. Besides, the sequence in which the various object sizes were measured was at random.

The results of all threshold determinations are reproduced in Fig. 3.2.3 and Fig. 3.2.4 for the glare and for the veil experiment respectively.

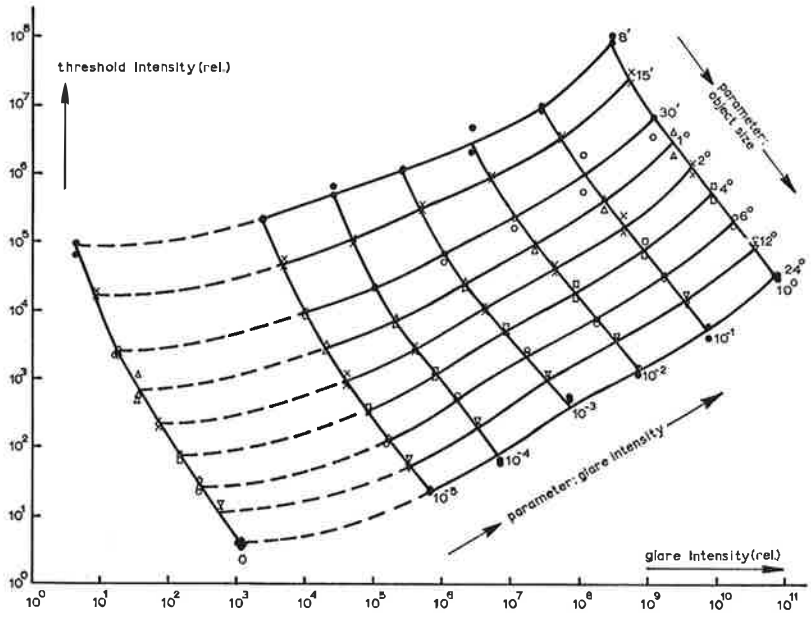

Fig. 3.2.3. The threshold of perception as a function of the glare intensity and the object size. The subsequent curves—with increasing object size—are moved over a factor 2 downward and to the right each time.

The method of plotting needs some explanation. Each "horizontal" curve represents a threshold / intensity relation for one object size. Each next curve is moved over a factor two, both down and to the right, with respect to the foregoing curve. This "quasi-stereo" presentation was chosen in stead of the more common presentation with an only vertical shift, because we can judge in this way the course of the threshold as a function, both of the masking intensity and of the object size. Now we are able to draw the connecting lines most accurately, closely fitting them to the experimental points on the one hand, and on the other hand making a regular network. Should all curves be identical, then the cross lines would be diagonals under 45°. The deviations from this 45° direction give us the dependency of the threshold upon the object size.

The simplest way to compare both figures and to get an overall impression of their similarity, is to hold them up to the light and to transilluminate them together. Typographical reasons preclude, that the reader actually can carry out this comparison himself here.

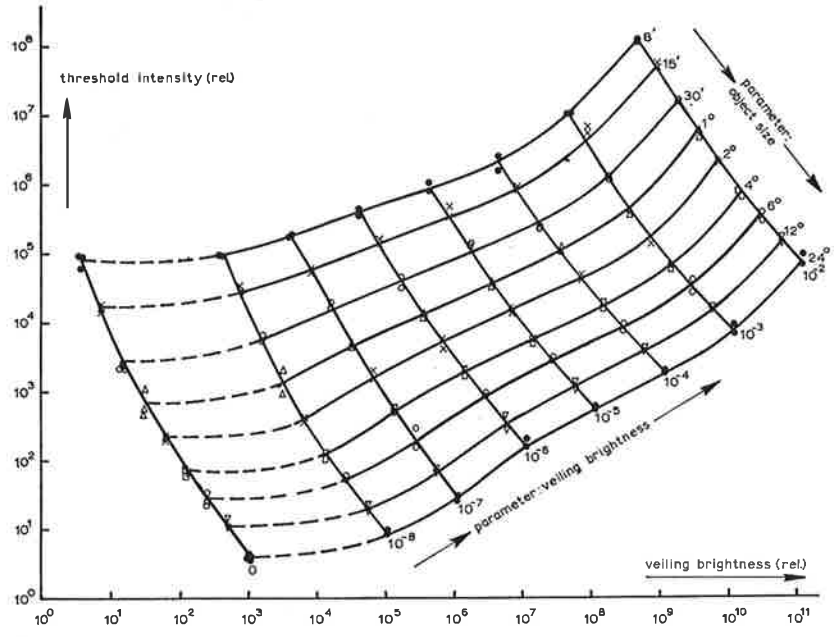

Fig. 3.2.4. The threshold of perception as a function of the veiling brightness and the object size. The subsequent curves—with increasing object size—are moved over a factor 2 downward and to the right each time.

This examination reveals, that the pictures have a good overall resemblance, though there are differences in details. The corresponding curves wind round each other, as it were. An obvious systematic divergence cannot be indicated, however. Especially the cross connections go nicely parallel, so that the dependency upon the object size seems to be quite the same in the glare and in the veil experiments. We further analyzed the differences quantitatively in many ways, but neither of them gave us a reason to change this first conclusion.

As an example, we present in Fig. 3.2.5, again in quasi-stereo presentation, the relation between B_{eq} and E for the various targets. If straylight should be the only determining factor, then the figure should be a nice rectangular framework: straight lines under 45°, moved over equal distances in the perpendicular direction. Deviations from this pattern reveal us the presence of alinear processes in a merciless way. The presence of such deviations cannot be mistaken. They seem to be restricted to the medium object sizes, which show a tendency to have a slightly smaller blinding capacity, especially at the lower glare levels. On the other hand, this effect does not affect the relation for the smallest and largest object sizes, which are practically identical apart

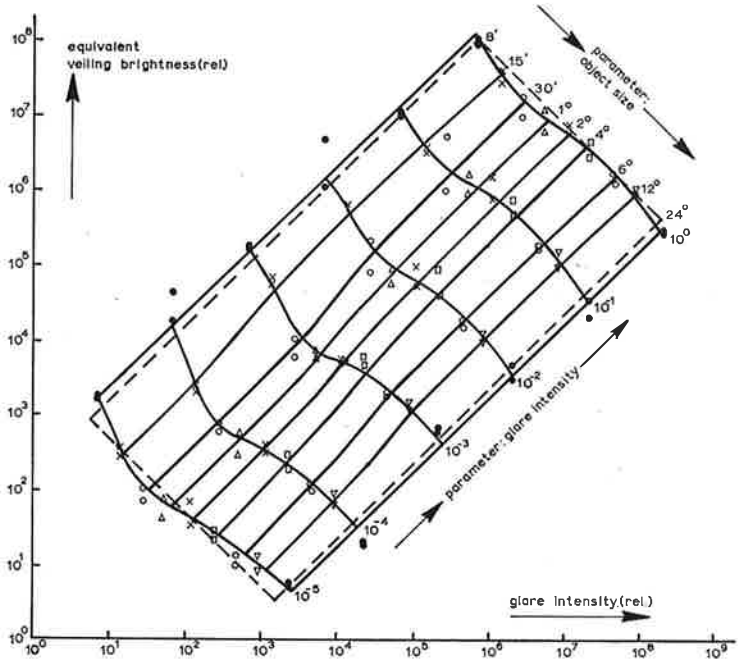

Fig. 3.2.5. The equivalent veiling brightness as a function of the glare intensity and the object size. The subsequent curves—with increasing object size—are moved over a factor 2 downward and to the right each time.

from the lateral shift. To illustrate this, we indicated the expected contour —expected on the basis of straylight only—of the frame with broken lines. The real figure hardly exceeds the expectancy limits.

Do we describe the equivalent brightness / glare intensity relations for the various target lengths by straight lines under 45°—and this is possible without much violating the experimental data—then we can characterize each of them by the blinding capacity (Form. 2.1.(1)):

Table 3.2.6

The blinding capacity for targets of various length

Target length	8′	15′	30′	1°	2°	4°	6°	12°	24°
Blinding capacity (rel.)	10	5.0	2.7	4.2	5.6	8.3	5.6	7.0	4.6

which table again shows no systematic gradient within the limits of its accuracy.

Therefore, the results described in these sections do not contain positive evidence about an influence of non-straylight action in glare. We have failed another time to demonstrate its existence.

3.3 Discussion

The experiments, described above, do not confirm the original conclusion of Bouman, that a glare source and an ectoptic luminous veil have a different influence on processes of neural adaptation. And this in circumstances, which we expected to work positively in favor of neural effects — if any. Yet the results are somewhat unsatisfactory, since the Fig. 3.2.3 and 4 do not cover each other completely in fine. We must assume, that the differences are caused by accidental errors — and remind the reader of the fact, that the procedure of construction of Fig. 3.2.5 gives a flattering picture of the real accuracy (§ 2.3). Besides, the difficult experimental circumstances — the small gap between the glare source and the target allows only very small deviations from a correct fixation — might partly explain the divergences. The origin of the divergence between our and Bouman's previous results remains unexplained. We can only point to a difference in the experimental circumstances (Bouman measured at a glare angle of about 2.5°).

Finally we should like to draw attention to the shape of the equivalent brightness curves (Fig. 3.2.5) once again. Similar curves from earlier experiments (Fig. 2.3.3) showed an inflexion around its mesopic range. Here, no systematic divergence from a linearity can be noticed, like can be seen from Fig. 3.3.1, in which all curves of the former graph are brought to mutual cover.

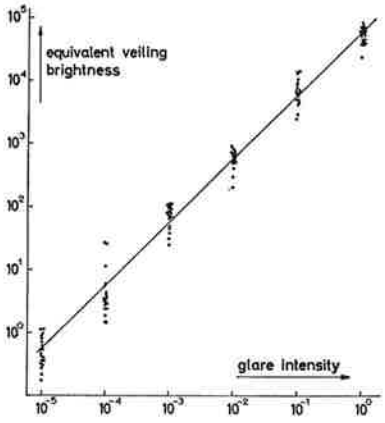

Fig. 3.3.1. The equivalent veiling brightness as a function of the glare intensity for all object sizes together. No significant deviations from a linearity are found.

It is difficult to explain the absence of the inflexion here and it will remain a difficulty, when we come to a discussion of the mechanisms of glare (§ 8.3h). We only mention here, that the situation differs from formerly by the eccentricity of the glare source (4° in stead of 0°), and by the smaller angle of glare.

3.4 Conclusions

The impossibility to indicate other causes of glare than entoptic straylight with certainty, invites for a reorientation with respect to the goal of our research. Taking for granted the dominance of straylight as a source of glare, we will study from now the sources of straylight in the human eye. The most interesting conclusion from the foregoing experiments is the unexpected influence of straylight originating from the fundus, as it became manifest in the jump of the blinding capacity at the transition from scotopic to photopic vision. We will in particular concentrate therefore upon the fundus component of entoptic straylight.

CHAPTER IV

BOEHM'S POLARIZATION BRUSHES

4.1 The phenomenon

In 1940 Boehm described a new[1] polarization phenomenon, which we will indicate as "Boehm brushes" in analogy with the more known "Haidinger brushes", with which they have something in common in appearance. We will survey his main findings.

Looking at a small light source, we see round about it the circularly symmetric veil, which is almost completely or totally due to entoptic scatter, like we have seen in the former chapters. When the light source is polarized, the veil gets a wing structure (Fig. 4.1.1) with its maximum intensity perpendicular to the direction of polarization.

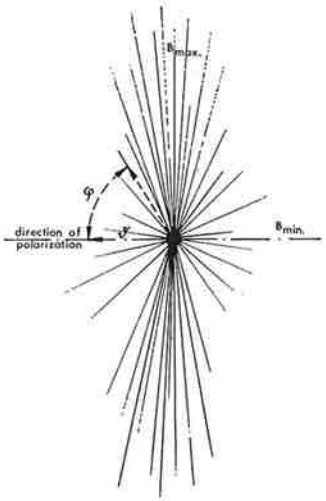

Fig. 4.1.1. Schematical representation of the appearance of Boehm brushes. The phenomenon is only visible, when the direction of polarization continually changes.

[1] Le Grand (1936) seems to describe a similar appearance and might be regarded as the discoverer proper, therefore. His inaccurate description of the Boehm brushes in his text book (1956) points to another way, however. Anyhow, Boehm was the first, who submitted them to a careful study.

The wings are only visible when the direction of polarization continually changes — like the Haidinger brushes — and they vanish as soon as it becomes stationary. They also disappear when the state of polarization is changed from linear via elliptic toward circular. Boehm used as a measure of their visibility the "threshold ellipticity", that is the ultimate ratio of the axes of the vibration ellipse, at which the brushes can be seen (ellipticity = 1 means circularly, ellipticity = 0 linearly polarized). This visibility threshold turned out to be hardly dependent on the color of the central light source (threshold ellipticity ≈ 0.8 for all kinds of light). Aphakes, color blinds and old people saw them as clearly as other people. The brushes were best visible, when the central source was seen in the near periphery of the field of view. They almost disappeared with central fixation or when the light source was focused on the papil.[1]

Boehm explained these phenomena by the scattering of light in the nervous plexus of the retina on the ground of the following strong and convincing arguments:

a. The influence of polarization in scattering processes only amounts to notable values for scattering angles round 90°. The scattering by the cornea and lens—the other main sources of straylight—is restricted to a narrow cone in forward directions ($\theta < 10°$ for the region in which the brushes are clearly seen) and the expected influence of polarization is small there.
b. The effect is independent of lens opacities (aphakes, old people), but strongly dependent on the place of the image of the light source on the retina. It is smallest, where the nervous plexus is thinnest: at the fovea.
c. Shadows of the retinal vessels, as they are produced by the well known method of retinal re-illumination (the so-called Purkinje vessels figures) are most distinctly visible in the direction, perpendicular to the direction of polarization of the direct fundus illuminations (Fig. 4.1.2).

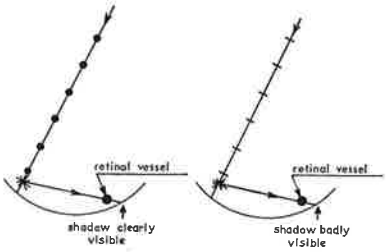

Fig. 4.1.2. The behavior of the Purkinje vessel shadows in retinal re-illumination, when the glare light is polarized.

[1] As to this point there is a marked contradiction between Boehm and Le Grand. The latter, in contrast, describes the effect for the papil, nota bene for the stationary image!

We should like to make the following notes. In the first place, it is evident that the Boehm brushes contain important information about the share of the retina in entoptic straylight, and that this process of scattering may not be neglected, such in agreement with our former findings (§ 2.3). Second, the method of the "threshold ellipticity" is only apt to study the relative visibilities in different, but comparable situations. It cannot be used to get information about the absolute amounts of straylight. Therefore, we have done some experiments, which were expected to give more quantitative data.

4.2 Photometry by imitation and compensation

Le Grand (1937) has shown, that it is possible to determine the brightness of a glare veil by the method of successive photometry. We felt this method not sufficiently accurate, however, to reveal small differences in brightness, like with Boehm brushes. We therefore took a slightly other way. We imitated the brushes in an artificial way and offered the Boehm pattern and the imitation brushes simultaneously to the observer, so that the brightness maximum of the imitation brushes coincided with the minimum of the Boehm brushes (90° mutual phase shift). The observer was asked to adjust the intensity of the imitation brushes so, that they just made the complement of the "natural" brushes; so that no wings could be perceived at all.

A schematic drawing of the experimental arrangement is given in Fig. 4.2.1. The field of view is represented by G. It consists of a ground paper screen on which the imitation brushes appear in projection round about a hole, through which the direct light from the polarized light source enters the eye. The observer looks at the fixation spot — again projected from behind — thus viewing the center of the Boehm brushes somewhere in the periphery of the field of view; or centric, according to choice. In our experiments, the observer used his right eye. Since the fixation spot was projected to the left of the hole, he always had the central light center projected in the region between the macula and the papil on the retina.

The arrangement consists of two light paths, which are brought together at the mirror M (with metallic surface reflexion to avoid non-wished polarization effects). L_b (the index *b* means "Boehm", *i* "imitation") is focused at M, the diaphragm D_b at the hole of G. The beam is polarized by the polaroid disc P, which slowly rotates (5 r.p.m.) in order to make the brushes visible.

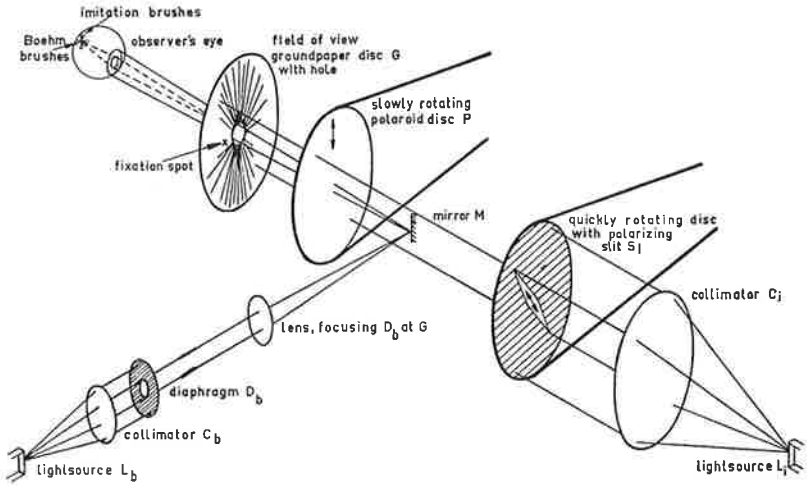

Fig. 4.2.1. The optical arrangement, to produce the entoptic Boehm brushes (index *b*) and the compensatory imitation field (index *i*).

L_i illuminates G through the polarizing, quickly rotating slit S_i and the slowly rotating disc P. One can understand, that S_i and P together produce the imitation brushes—as indicated at G—as soon as S_i has a speed of rotation beyond the flicker fusion limit. The wings of the imitation brushes stand parallel with P, perpendicular therefore to the Boehm brushes automatically. The tapering shape of S_i provides a rapid fall of the intensity of the imitation brushes with increasing distance to the central light source.

The observer perceives, apart from the fixation spot, a polarized intensive light source, its accessory Boehm brushes and the imitation brushes. This ensemble slowly rotates about 5 times a minute. When the imitation brushes are faint, the real brushes predominate and we perceive the bright wings perpendicular to the polarization of P (wings "out of phase"). When the imitation brushes are intensive, the Boehm brushes are overcompensated: the imitation brushes now predominate and we perceive the wings in phase with P. Somewhere between is the exact compensatory position, in which neither the Boehm, nor the imitation brushes predominate and no wings can be perceived at all. The determination of the right compensation was performed in the following way. The operator ajdusted the currents through the lamps L_b (constant during each session) and L_i at some feasonable values and the subject judged at which moments the bright wings of the scene passed through the horizontal position. With counters and sliding contacts was recorded, whether he pressed the

key "in phase", "out of phase", or somewhere between. Ten key pressings gave one value for the "chance to see the Boehm brushes dominant". About ten chance values for various intensities of L_i (measured in random sequence) together constituted one "frequency of seeing curve". The 50 % chance value, finally, gave the compensation intensity of L_i. An example of such a chance curve is given in Fig. 4.2.2.

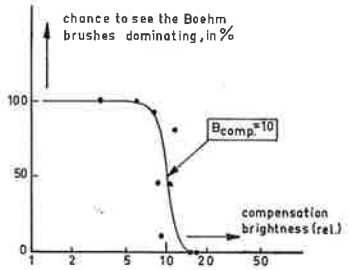

Fig. 4.2.2. The change in dominance from the entoptic Boehm pattern to the ectoptic compensation pattern with increasing brightness of the latter.

In a given glare situation, the brightness of the Boehm brushes will be represented by

$$B_b = B_1\ (\vartheta) + B_2\ (\vartheta)\ \sin^2 \varphi, \qquad (1)$$

in which B_1 represents the non-polarized part of the entoptic veil and B_2 the polarized part. φ is the phase angle with respect to the plane of polarization (Fig. 4.1.1). For the justification of (1), we refer to § 7.3. The compensation brushes are characterized by

$$B_{comp} = B_i\ (\vartheta)\ \cos^2 \varphi, \qquad (2)$$

in which B_i was designed to resemble B_2 (tapering slit), so that it should be able to fill up B_b over the full field of view. Of course, the compensation is never complete, as the imitation brushes not exactly resemble the original. Especially in the neighborhood of the center, the imitation brushes are too faint due to the finite width of the slit S_i. Therefore, the observer was instructed to search for the right compensation on the ground of the overall structure of the whole field and not on the ground of local circumstances around the point of fixation or in the direct environment of the glare source. The proof of the pudding is in the eating, and so here, the reproducibility of the compensation adjustment (Fig. 4.2.2) is an indication that the imitation was not so bad at all.

4.3 Results of the compensation experiments

In order to plot our data in a simple way, we introduce the "ripple ratio"

$$r = \frac{B_{max} - B_{min}}{B_{average}} \tag{1}$$

It represents the brightness modulation, caused by the alternation of bright and dark wings. The compensation brushes just fill up the dark gap, so that $B_{max} - B_{min} = (B_{comp})_{max} = B_i$. Thus:

$$r = \frac{B_i}{B_{av}} \tag{2}$$

Its value is simply determined from the adjustment values I_i of L_i and I_b of L_b.

a. As the compensation was supposed to be complete over the whole field, we determined r at one eccentricity only. This point was chosen at an arbitrary medium distance from the center, at 3.4°.
b. The value of B_i at that place was 2.4 cd/m² in white light, at the maximum voltage of L_i. This value was determined by flicker photometry.
c. As a result we have

$$B_i = 2.4\ \tau_{color}\ I_i \text{ cd/m}^2 \tag{3}$$

in which I_i represents the relative intensity of L_i—relative with respect to its maximum value—and τ_{color} the transmission of the color filter.
d. The brightness of the total veil of straylight (B_{av}) is known from other psychophysical experiments (Table 2.3.5) and amounts about

$$B_{av} = 10\ E / \theta^2 \cdot \tau_{color} \cdot I_b \text{ cd/m}^2 . \tag{4}$$

Flicker photometry gave for the glare intensity E the value of 15 lux (in white light) so that for $\theta = 3.4°$:

$$B_{av} = 13\ \tau_{color}\ I_b \text{ cd/m}^2 . \tag{5}$$

e. The value of r is obtained by dividing (3) and (5).

We find:

$$r = 0.18\ \frac{I_i}{I_b} . \tag{6}$$

It is in terms of r, that we plotted the experimental results in Fig. 4.3.1 as a function of the eccentricity of the glare source in the field of view and for four different colors of the glare light. Ordinary glass absorption filters were used to obtain these colors. The presented graphs are measured by one subject (the author). Another subject measured a series in green light only. His results did not notably differ from those presented here.

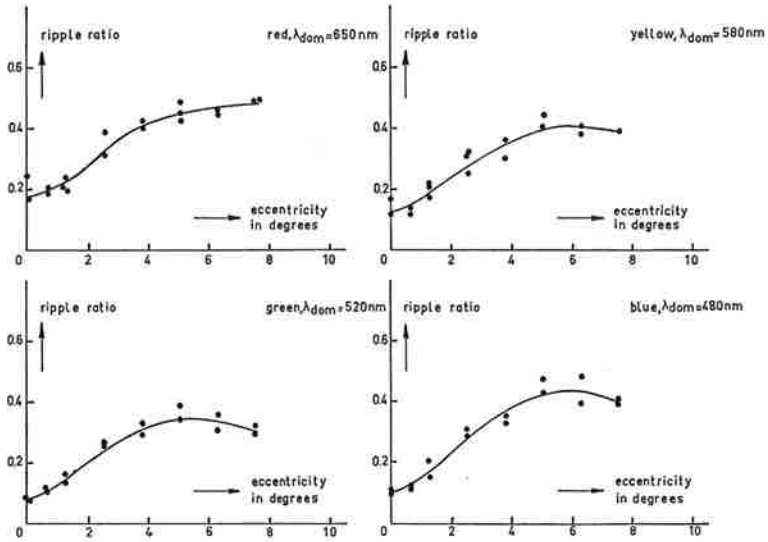

Fig. 4.3.1. The dependency of the ripple ratio r = relative difference in brightness between the bright and the dark wings of the Boehm pattern, as a function of the eccentricity of the glare source in the field of view.

In the first place we note the general mutual resemblance of the four curves, which means that the wavelength dependency is small. Second, r notably rises from centric to eccentric fixation, but seems to reach some saturation beyond 4°. This behavior has some resemblance with the course of the thickness of the retina with increasing distance from the foveal center, and our measurements might be regarded as a corroboration of Boehm's concept of the origin of the brushes.

Finally, we are surprised by the height of the ripple ratio attained. More or less intuitively, we had expected values of some 10 % at most, thinking of the invisibility of the brush pattern in the stationary situation. The present experiments reveal, that the polarized part amounts to some 40 % of the total entoptic veil, so that we must assume that the retina notably contributes to the process of intraocular scatter.

4.4 Photometry by threshold determinations

In the former section, we concluded, that the Boehm brushes were characterized by a much larger ripple ratio than was expected. This

new situation opened other ways for investigation. The difference between the maximum and minimum brightness seems to be enough to give measurable differences in contrast thresholds and so we can explore the straylight veil more locally and more accurately by the formerly used "equivalent veil" method (Ch. II).

The experiments were carried out with the equipment, amply described before (§ 2.2, Fig. 2.2.1), which had to undergo some minor modifications only. The lower lightpath — serving for the glare beam / veil brightness — was polarized by insertion of a polaroid sheet, mounted at S. It could be given any desired position by rotation. G and M_2 give some polarization too, and the combined influence of these mirrors, together with the polaroid sheet might give some parasitic brightness modulation. Therefore G was removed (the fixation spots were directly applied at the object diaphragm). With M_2 we could not dispense and the experiments had to be corrected for its disturbing influence. With this equipment, the experimental situations were produced, which are shown in Fig. 4.4.1.

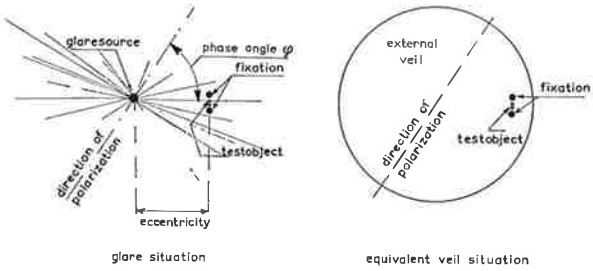

Fig. 4.4.1. The experimental situations investigated. The eccentricity of the glare source in the field of view and the phase angle could be varied.

The object was presented just between the two fixation spots, which could be chosen at various eccentricities in the illuminated field: at 2.3°, 3.8°, 4.6° and 6.1°. All experiments, the glare as well as the veil experiments, were performed with four values of the phase angle (0°, 30°, 60° and 90°), so that 4×4 conditions were investigated. The equivalent veil was determined in the usual way, be it that we needed only one threshold value under the condition of glare and a small part only of the threshold versus brightness relation under veil conditions.

The experimental technique was the same as described in § 2.2, with the difference only, that we had taken some additional measures

to eliminate the influence of bias. In the first place, the experiments were performed by two persons now: one as subject (the author), the other as operator. The operator did not inform the subject about the results before the experiments were completely finished. And second, neither the subject, nor the operator knew the position of the polaroid sheet in its holder during the experiments: it was only determined afterwards.

As mentioned before, some influence of polarization can be expected by reflexion at M_2, and other, not always exactly perpendicular or centered surfaces. This effect can easily be read from the dependence of the threshold on the phase angle in the veil experiments (Table 4.4.2, second line). Since these thresholds were determined eccentrically in the field of view and we had to correct for variations in the glare intensity too, we additionally performed some threshold determinations in the very center of the luminous field, at the place of the glare source (third line). These results are qualitatively well in accordance with what we could expect on theoretical grounds (last line, $1 + p \cos^2 \varphi$, with a best fitting value of p). The value $p = 0.28$ seems not to be excessive in view of the many air/glass surfaces which have to be transmitted. The equivalent brightness and the glare data, have been corrected with the second and third line values respectively.

Table 4.4.2

The influence of parasitic polarization effects in the apparatus on the threshold of the test object

Phase angle φ	0°	30°	60°	90°
Relative threshold in veil experiments (all eccentricities together)	1	1.17	1.33	1.36
Relative threshold in veil experiments (eccentricity zero)	1	1.09	1.20	1.28
$1 + 0.28 \cos^2 \varphi$ (best fitting theoretical course)	1	1.14	1.21	1.28

The final results of the measurements are presented in Fig. 4.4.3. The four separate graphs give the equivalent brightness as a function of the phase angle for the four eccentricities of the glare source investigated.

According to our expectations, there is some general tendency toward a higher equivalent brightness at 90° (bright sector of the Boehm brushes) than at 0° (dark sector), but the spread of the individual points is too large, to judge possible differences between the four graphs.

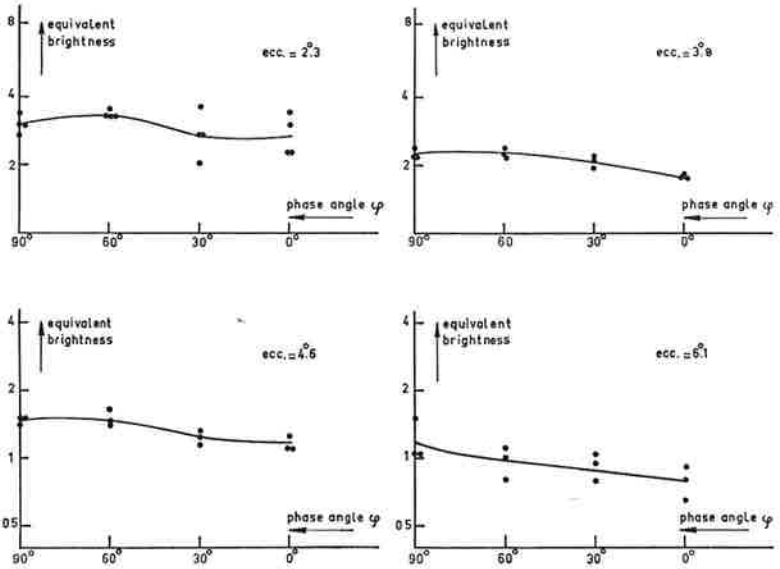

Fig. 4.4.3. The equivalent brightness of the entoptic veil round about a white polarized glare source as a function of the phase angle φ with respect to the direction of polarization. The four curves are determined at various angular distances from the glare source.

In order to study the general trend more accurately, we brought the graphs to mutual cover in Fig. 4.4.4, and drew the best fitting curve $a + b \sin^2 \varphi$, viz. $0.81 + 0.19 \sin^2 \varphi$.

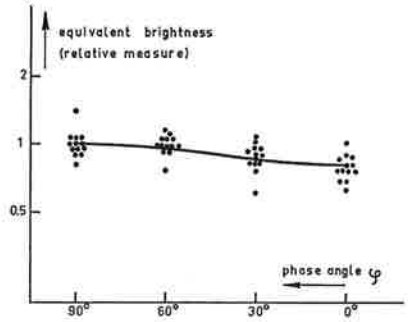

Fig. 4.4.4. The same relation as in fig. 4.4.3, now with all graphs brought to mutual cover. Drawn: the best fitting theoretical curve: $B_{eq} = 0.81 + 0.19 \sin^2 \varphi$.

As a consequence, the ripple ratio derived, is $\frac{b}{a + \frac{1}{2} b} = 21\ \%$ with an inaccuracy of $\pm 5\ \%$.

This ratio is of the same order of magnitude as, but definitely lower than the previously found value ($\approx 40\ \%$). However, the experimental conditions are not fully comparable. In § 4.3: perception with the whole periphery, with as criterion a more or less integrated impression; and here: perception with the fovea centralis. In how far these factors may influence the results will come up for discussion in the last chapters.

CHAPTER V

THE STILES-CRAWFORD EFFECT IN GLARE

5.1 The basic idea

In 1933 Stiles and Crawford described their discovery, that the luminous efficiency of a narrow beam of light changed with the point of entry at the pupil. The maximum efficiency is usually found near the pupil center, but near the margin of a large pupil it is lowered by a factor 5 to 10. It is generally assumed now, that this "Stiles-Crawford effect" is due to the directional sensitivity of the cones (the effect is absent or nearly absent in scotopic vision), which are properly parallel implanted in the retina, approximately directed toward the pupil center.

This mechanism of directional sensitivity necessarily must discriminate between straylight evoked in the anterior eye media like cornea and lens, and straylight originating from the fundus. The first kind will gradually decrease in masking efficiency with increasing eccentricity of the entrance of the glare beam at the pupil, whereas the angle of incidence of the fundus straylight will remain unchanged — and thus its visual effect. Therefore we can expect: the greater the share of the fundus in entoptic straylight, the smaller the influence of the place of entry on the veiling capacity of a glare source, the larger the difference in Stiles-Crawford behavior between a glare veil and an ectoptic masking veil. And the reverse: from that difference in Stiles-Crawford behavior we can read the share of the fundus in entoptic straylight. This is the very aim of this chapter.

5.2 Procedure and results

The experiments were carried out with the apparatus of Fig. 2.2.1 and essentially following the procedure, described in § 4.4. In order to obtain a sufficient accuracy, the entrance pupil was reduced to 0.5 mm diameter. The change in the place of entry at the pupil was performed by moving the head (rest). In this way both entering

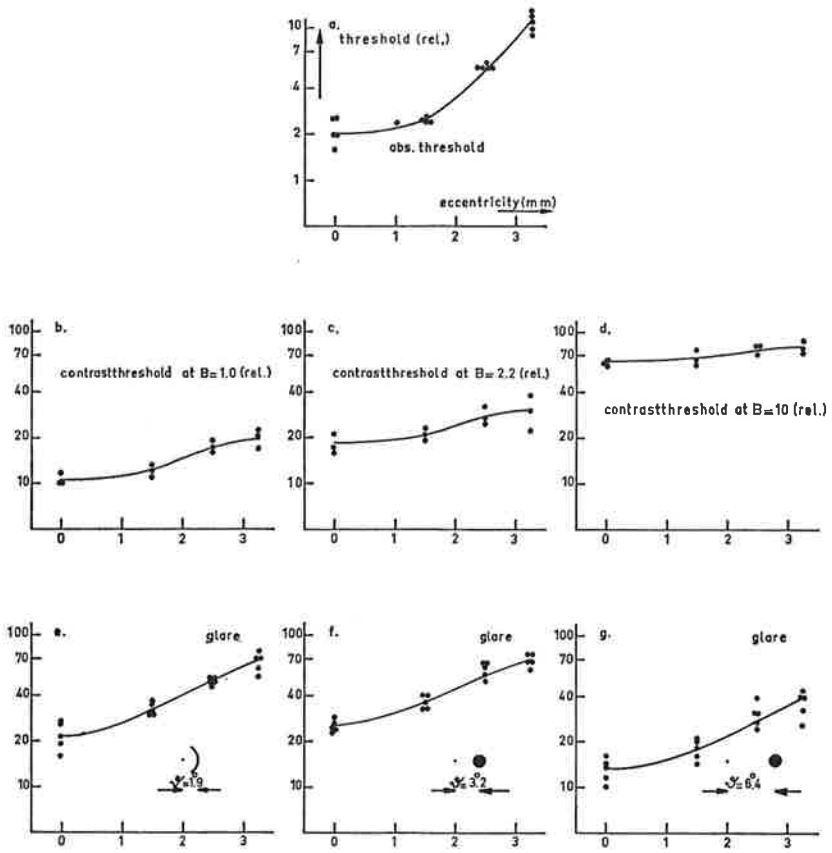

Fig. 5.2.1. The change in the threshold of perception with the eccentricity of both the test and the mask beam. *a:* The absolute threshold shows the well known Stiles-Crawford effect. *b, c, d:* The effect disappears in contrast threshold experiments, when the Weber-Fechner domain is reached ($\Delta B/B = \eta \Delta B/\eta B$). *e, f, g:* In glare situations, the Stiles-Crawford effect only partly disappears, because the fundus component does not decrease in luminous efficiency.

beams (glare/veil and test object) changed their place of entry, but this did not matter for the final result, because the test object has a mediator's role only. There was no special device to control the position of the pupil with respect to the incident beams. However, the shadow of the iris, as it was projected on the retina from the cornea as a scatter center, formed a clear and, as appears from the reproducibility of the experimental results, sufficient indication of the right centration, both in glare and veil experiments. We could notice that the head fixations formed an extremely efficient and accurate fixation

tool, which could be fairly trusted, even in the absence of visual fixation aids.

The scene was as follows: the test object was presented foveally in red light, and the glare source (white) at various angular distances in the near periphery. The flash time was 0.5 seconds. The results of the experiments are presented in Fig. 5.2.1, the scenes are schematically indicated as insets. The upper graph gives the absolute threshold as a function of the eccentricity of incidence at the pupil, and thus shows the pure Stiles-Crawford effect. The row below gives, in the same way, the contrast threshold at some luminances of the ectoptic veil. We note a reduced effect of the eccentric beam entrance, because the final effect is a compromise between the Stiles-Crawford effect of the test flash and of the masking veil. In the Weber-Fechner domain they completely neutralize each other: an equal reduction in luminous effect of both the masking veil and the test flash does not affect the threshold situation at all. The lower row, finally, gives the increase of the threshold in three glare situations. The glare intensities in the three situations were chosen in such a way, that the threshold values lie at about the same level as the thresholds in the equivalent veil experiments.

The divergence between the glare and the veil curves is obvious.

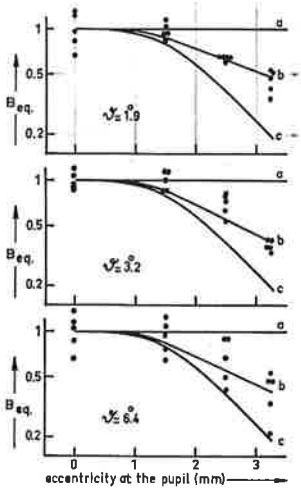

Fig. 5.2.2. The decrease in brightness of the entoptic glare veil with increasing eccentricity of the entrance of the glare beam at the pupil. Curve *a* should be expected if all entoptic straylight came from the fundus, curve c if all came from the cornea and the crystalline lens.

In order to study this divergence in a quantitative way, we converted these curves into equivalent veil relations in the customary way. We get then equivalent values for a veil, focused at the retina via the same eccentric entrance as the glare beam. We must therefore convert these values again — now with the absolute threshold curve — for the reduced luminous efficiency at this eccentricity. In this way, finally, Fig. 5.2.2 has been brought about.

Should all straylight come from the fundus, then no reduction of the equivalent veil should be expected (curve a). Should all straylight come from the cornea and the lens, then the reduction in the luminous efficiency should be felt fully (curve c). The experimental curves lie between both curves. They are drawn as the best fitting theoretical curves. Here theoretical means, that the curves are drawn as proportional reductions of curve a to c. This is not directly evident from the figure, because of the logarithmic way of plotting. One can easily verify that the

$$\text{relative share of the fundus} = \frac{b - c}{a - c} \qquad (1)$$

and in this way we find: for $\vartheta = 1.9°$ a share of the fundus of about 35 %, for $\vartheta = 3.2°$ a share of some 25 %, and for $\vartheta = 6.4°$ a share of about 25 %. The accuracy of these figures is not very large of course. We have performed this type of measurements a number of times with small variations in experimental circumstances only, just because we thought them really marginal experiments. The results shown here, were the best qua experimental technique and representative for the average results.

In fact the fundus shares found ranged between 10 % and 60 %. Concluding we would say, that the experimental findings clearly point to a fundus share of the order of 30 %, but that we dare not differentiate as to the glare angle.

5.3 Discussion

The foregoing results are derived under the silent assumption that the scattering properties of the lens and the cornea are not dependent on the place of entrance of the glare beam. However, a decrease in the amount of straylight from these anterior eye media with increasing eccentricity might have a reducing effect on the equivalent veiling brightness as well, but in a much simpler way. Therefore we performed a test trial. The experiments were repeated, now with the

glare source presented foveally and the test object as a ring around — in short: the same arrangement as in Chapter II. Moreover, the test object was presented at λ = 480 nm, so that rod vision only was involved.

The results of these experiments can be found in Fig. 5.3.1 for glare and veil both. They show no dependency at all on the eccentricity of incidence. That the veil experiments show no effect confirms, that we measured a rod effect indeed; that the glare curves are straight horizontals can only mean that the total amount of entoptic straylight is independent of the eccentricity of incidence.

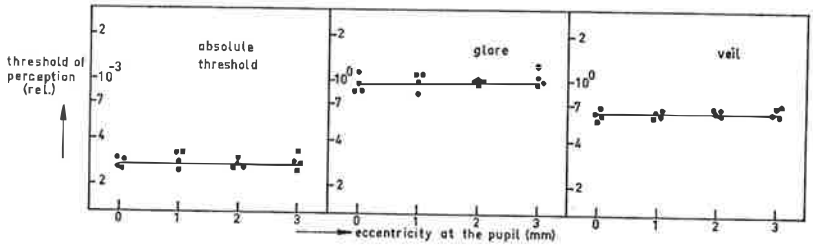

Fig. 5.3.1. The absence of a change in threshold with the eccentricity of entrance at the pupil at scotopic perceptive conditions, even in the glare situation, demonstrates, that an eventual decrease in the scatter contribution of the lens toward the iris border plays no role of significance.

We can draw two conclusions. First, we are justified now to use the unchanged value of 30 %, deduced in the former section for the fundus share in entoptic straylight. But second, the results of Fig. 5.3.1 give us some information about the lens scattering. We can understand — looking at the slitlamp photograph (frontispiece) — that the cornea and external lens capsules give a constant contribution to entoptic straylight all over their surface as a first approximation. The thinning of the lens interior, however, must have an effect in principle. That we did not find an effect, means that the scattering capacity of the lens core is relatively small, also in forward directions.

CHAPTER VI

SHADOW CASTING THE IRIS

6.1 Purpose and method

When a glare beam enters the eye as a tiny pencil of light, the cornea becomes a pointolite source of straylight. This straylight transilluminates the pupil and casts a shadow of the iris on the retina (Fig. 6.1.1). We perceive it as a faint light circle on a dark background in the far periphery of the field of view. In the former chapter, we used this shadow figure as a tool for centration only. Here we will make it subject of investigation itself: we will try to measure the brightness jump at its border. This jump, the difference between entoptic straylight with and without participation of the cornea, will give us the share of the cornea in entoptic scatter.

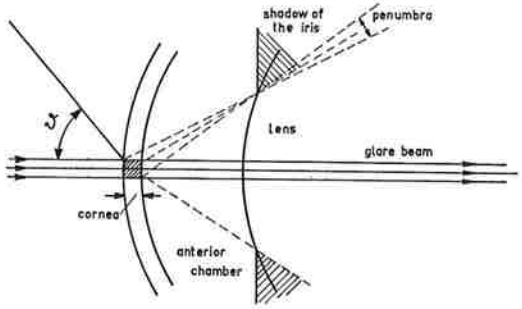

Fig. 6.1.1. The translighting of the iris by the corneal scattering. The width of the pupil determines the size of the entoptic light circle on the retina, which corresponds with the angle of glare in the visual field.

In 1958 DeMott and Boynton separated, for excised eyes, the entoptic straylight in its constituent parts by photographing the interior of the eye through a pinhole at the posterior pole of the eye ball. They found, that some 70 % was due to the cornea (almost independent of the angle of glare) and about 30 % to the crystalline lens and the anterior chamber. Against this conclusion two serious objections might

be raised. First, the fundus remission was left out of account, so that these percentages only hold for the non-fundus share. On the ground of our knowledge now, we might expect a clear reduction of these percentages. And second, the study of excised eyes always is a precarious business in view of the rapid post mortem changes, especially of the cornea. It speaks volumes, that Boynton found, in earlier but similar experiments with Enoch and Bush (1954), a ten times higher amount of straylight than could be expected from psychophysical experiments. In the experiments of 1958, the contribution of the anterior chamber raises suspicion: in slit lamp examination it is usually found optically empty. A psychophysical determination of the corneal share in entoptic straylight would be a control on DeMott and Boynton's data and a welcome addition to our knowledge after our investigations on the fundus remission.

The way, how to measure the brightness jump between the light circle and the shadow is a problem itself, because of the far peripheral position of the jump in the field of view (between 30° and 70°, depending on the pupil diameter).

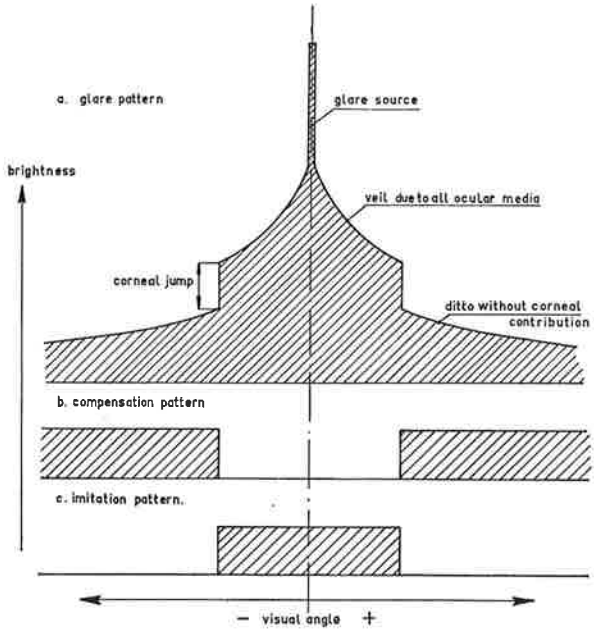

Fig. 6.1.2. The brightness distribution in the entoptic veil round about the glare source (a). The jump at the shadow border is either compensated by the pattern (b) or imitated by the pattern (c).

We chose a method of compensation and one of imitation (Fig. 6.1.2). In the compensation experiments, a dark circle on a uniform background was added to the glare pattern. Its size and brightness were adjusted so, that the corneal jump was just compensated. In the imitation design, the glare pattern was compared with a white circle on a dark background; size and brightness of the latter were adjusted so, that their jumps seemed to be equal. The real course of things will be explained in the next section.

6.2 Experimental technique

The experimental technique will be described on the basis of Fig. 6.2.1. The observer looks at the lens L, which is the only object on a structureless white screen. The lens concentrated the glare beam on the cornea (Maxwellian view principle; cross section at the cornea 0.3 mm). The compensation and imitation pictures — shortly: "projections" — are focused on the screen from the other side.

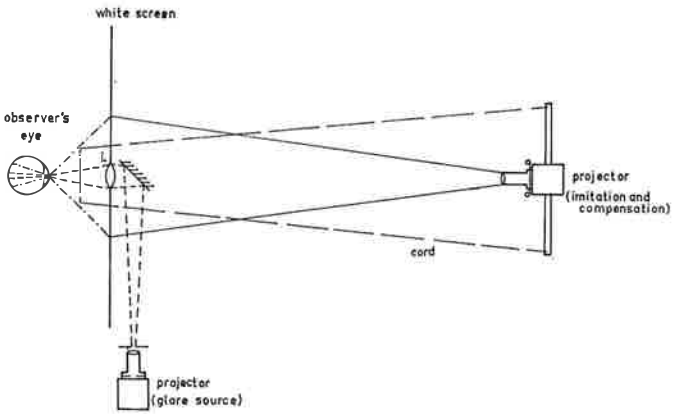

Fig. 6.2.1. The optical arrangement. The field of view consists of the lens L, providing the glare source in Maxwellian view, and the white screen, on which the imitation and compensation circles are projected from behind. With the cords, the subject can give the projections small shaking movements, which imitate the effect of eye movements on the glare pattern.

Steady objects in the periphery of the field of view tend to fade out. This problem is easily and more or less automatically solved for the iris shadow, as small eye movements, such as usually occur, again and again do reappear it.

In order to get equivalence between the glare picture and the projections as far as possible, we gave the observer two cords toward the projector, which allowed him to give the projection small shaking movements as well. As a result, the observer does not see the glare pattern and the projection coincident. Phenomenologically described, he successively compares two wobbling structureless light circles as to their size and to the pregnancy of their edges. That is why he does not feel much difference between the imitation and the compensation experiments, though the visual tasks might look entirely different from a physical point of view.

That one really matches the border jumps — and not some overall brightness — was verified in a few test experiments with two projections: the original one, and another, quite similar in presentation, but with a strong fall in brightness toward the edge. Either of them could be moved independently in the way, described above. In fact, the border jumps appeared to be equalized in these experiments.

The procedure proper was as follows: the experimenter adjusted some brightness value of the projection and the observer reported "projection dominant", "equal", or "glare dominant". He could discern both circles by whether they reacted on head or eye movements. On the whole, this procedure was similar to that, reported in our description of the first type of Boehm experiments (§ 4.2). There is another similarity yet: the unexpected reproducibility of the results, quite comparable with those obtained in Fig. 4.2.2. We know, that there is not a sudden jump in brightness, but a penumbra which subtends some 10° visual angle. That this gradualness of transition does not give rise to large incertainties must be ascribed to the small separating power of the peripheral retina. In fact, the penumbra is hardly perceived as such, especially at large pupil sizes. We must add, that the accuracy above mentioned, was only reached by two observers. A third one, experienced like the others, did not succeed to get a match between the two pictures at all.

6.3 **Results**

The results for the two observers are reproduced in Fig. 6.3.1, where the brightness jump, due to the screening of the corneal straylight, is plotted against the angle of glare. The experiments were done for various sizes of the pupil. The size of the pupil was regulated

by instillation of mydriatics and miotics. In this way, we could vary the size of the light circle, or, in other words: the angle of glare. For the sake of comparison, the relation $B = 10\ E / \vartheta^2$, the average course of the equivalent veiling brightness, as it is derived from psychophysical experiments (Table 2.3.5), and DeMott and Boynton's curve, brought to the same level, are given by the drawn and the interrupted curve respectively. In order to draw the $10\ E / \vartheta^2$ curve, we have to know the value of E. This always gives some trouble in optical arrangements using the Maxwellian view arrangement. The incident luminous flux was 7×10^{-4} lm (determined by flicker photometry), the size of the natural pupil at this glare level was 6 mm for both observers (determination by flash photography). The effective value of E can now be computed by taking:

$$= \frac{\text{luminous flux} = 7\times10^{-4}\ \text{lm}}{\text{natural pupil area} = \pi/4.\ (6\times10^{-3})^2\text{m}^2} \cdot \frac{1}{\text{average luminous efficiency of the pupil} \approx 0.6} = 40\ \text{lux}.$$

We notice:

a. The reproducibility and the agreement between the imitation and the compensation experiments is satisfactory.

b. The results of both subjects agree qua general level, but they diverge at the large angle side. Where we have no reason to assume notable differences in the corneal scattering properties, we are inclined to impute this to the incertainties in the direction of the abscis of Fig. 6.3.1, caused by the width of the penumbra. For clearness' sake we indicated, by arrows, this width in the figure. We take this discrepancy as an extra warning, that this method is a rough approximation only and that details cannot be used as a base for interpretation.

c. A comparison between the general levels of the cornea curve and the curve for the total entoptic veil brightness must be done with due reserve, because of the uncertainty in the absolute height of the latter curve. The given course is determined on other subjects and with the glare source eccentrically in the field of view, and so it can only be considered as a rough approximation.

Considering now the final results, we notice that the general behavior of our corneal data and of the full equivalent veil curve is more or less the same in the range studied, with a small tendency to a steeper cornea curve perhaps. The cornea share seems to be some

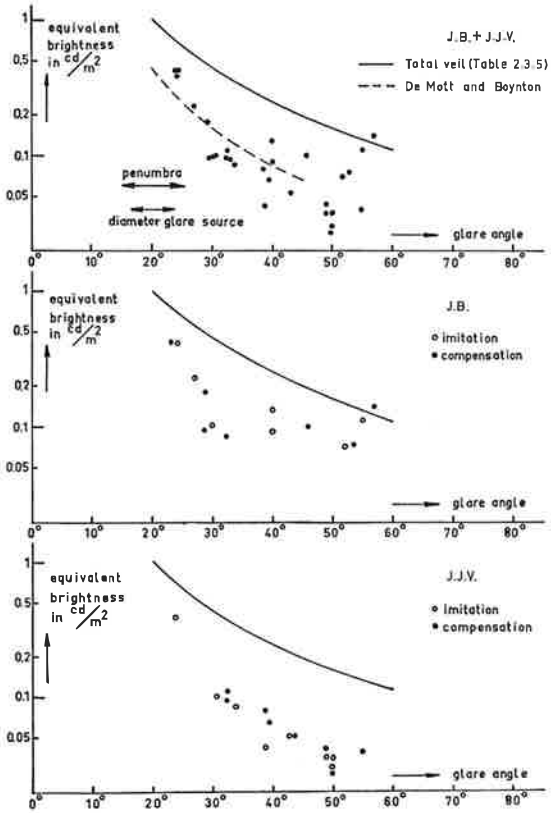

Fig. 6.3.1. The equivalent brightness of the corneal contribution to the entoptic veil as a function of the angular distance to the glare source. As a comparison, we drew the curve for the total entoptic veil according the literature data and, interruptedly, the course of the cornea component according to DeMott and Boynton, brought to the same level as the experimental points.

30 % [1] (average ratio of the experimental point level, to the drawn curve for the total entoptic brightness in Fig. 6.3.1a). We will subject this figure to further discussion in the final chapter.

[1] After the completion of the manuscript, we found this figure confirmed by Boynton and Clarke (1962), who seem to have used a similar technique.

CHAPTER VII

MECHANISMS OF FUNDUS REMISSION

7.1 Introduction

In the former chapter more and more evidence has been produced, that the fundus remission forms an important part of the intra-ocular scattering.

We did not find this explicitely stated in the literature, and its rather complex mechanism seems never to have been analyzed in detail. This now has been the goal of the investigations, described in this chapter.

In our opinion, three types of fundus straylight should be discerned (Fig. 7.1.1):

a. Straylight evoked in the nervous tissues of the retina — which we will indicate as "retinal straylight" (§§ 7.3,4).

b. Straylight coming from the pigment layer just behind the retina — which we will call the "pigment reflexion" (§§ 7.5,6).

c. Straylight evoked behind the retina by reflexion at the sclera — which we will call the "scleral reflexion" (§§ 7.5,7).

We will also pay some attention to the corneal reflexion of the fundus image, which will be shown to be only of minor interest (§ 7.8). Of course, we will have to make assumptions about the receptive mechanism of rods and cones at these unusual angles of incidence (§ 7.2) and about the scattering mechanisms involved. With the help of the available data from anatomy and physics, we will construct a model and compute the equivalent veiling brightness in various circumstances of glare. Although this model should be considered as a first approximation only, we will prove anyhow, that there is a set of assumptions, not incompatible with the data from anatomy or physics, which might explain most experimental data.

The discussions in the next sections will mainly concern details, so that the outlines might be lost. Therefore, we will finish this chapter with a review, in which we will resume the central points.

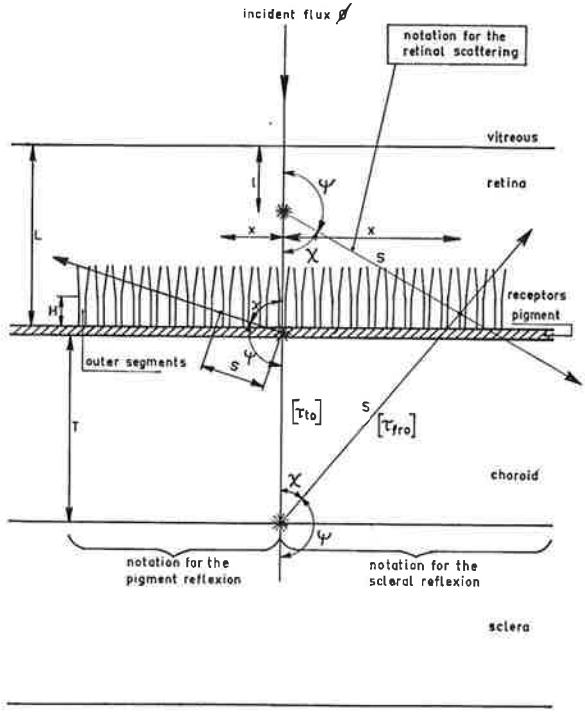

Fig. 7.1.1. The stratification of the fundus with a survey of the notations, used in the various sections of this chapter.

7.2 The receptive mechanism

It is not primarily the retinal illumination (E) which is of interest for us, but its luminous effect (ε). Since the discovery of the Stiles-Crawford effect we know that the luminous effect is not independent of the direction of incidence of the rays at the retina, at least in cone vision. What we are particularly interested in, is the behavior of the luminous efficiency η at large angles of incidence, such as occur in fundus straylight. No experimental data are available, but we know the responsible mechanism: the grazing incidence reflexion in the funnel shaped inner segments and in the outer segments of the cones. On the ground of simple geometric-optical laws, we may expect that this catching mechanism rapidly decreases in importance with increasing angle of incidence and is completely outruled for angles beyond, say 45°. Beyond this angle, the luminous efficiency will hard-

ly change any more. In rod vision, the Stiles-Crawford effect seems to be absent or of minor importance only.

Let us assume that the amount of light, absorbed in the photopigment, is a minor fraction only of what is incident. Then, the perspective shortening of a given retinal area with increasing angle of incidence is compensated by the lengthening of the effective pathway through the absorptive layer, so that the same retinal illumination (in lux e.g.) will give rise to the same luminous effect (in numbers of excitation per unit of area), independently of the angle of incidence. The transparency of the retina is a sufficient justification for the basic assumption only, if the pigment is distributed homogeneously over the retina. This condition is satisfied for large angles of incidence, when each ray passes through several receptors. But with perpendicular incidence, some 80 % absorption might even be expected in each individual cone receptor, like Walraven and Bouman (1960) derived from the wavelength dependence of the Stiles-Crawford effect. Apparently, the assumption of transparency does not hold for perpendicular or nearly perpendicular incidence. But exactly at these angles, we met already an anomalous behavior in the Stiles-Crawford effect. It appears from the above cited paper (see also Walraven 1962), that the influence of the high density can effectively be described by a slight reduction of the Stiles-Crawford effect, expected on the ground of the funelling effect only. Effectively, we can say that the receptive layer acts as a transparent absorbens in all directions but the forward. In these directions it is preferentially sensitive according to the experimentally found Stiles-Crawford effect.

There is a second effect, which influences the efficiency of the receptive mechanism, namely the orderly arrangement of the visual pigments. In rods — and why should not the same hold for cones? — they are arranged with their dipole moment perpendicularly to the receptor axis and they have a preferential direction therefore, for normally incident light (Denton 1957). As a consequence, natural light incident at 90° — that is: parallel to the retina — has only half the luminous effect of natural light with normal incidence. Generally we can say, that the component vibrating parallel to the retina has a luminous efficiency which is independent of the angle of incidence, whereas the other component, vibrating in the plane through the incident ray perpendicularly to the retina, decreases in efficiency with $\cos^2 \chi$, in which χ is the angle of incidence of the scattered light with the normal (Fig. 7.1.1).

A part of the fundus straylight is almost completely polarized, namely the retinal component (see § 7.3). Its plane of polarization is parallel with the retina, however, so that the luminous effect does not differ from perpendicularly incident light. Other components (the pigment and the sclera reflexion) will turn out to be almost completely depolarized (§§ 7.6,7). This means, that one half of them must be subject to this $\cos^2 \chi$ law.

Summarizing and rounding the picture now, we get:

For perpendicularly incident light: $\eta = 1$ per definition, independently of the direction of polarization. For large values of χ: $\eta// = p$ and $\eta\# = p \cos^2 \chi$, in which the index // means: polarization parallel to the retina, # indicates the perpendicularly polarized component and p represents the inverse of the effective funelling factor, which O'Brien (1951) estimated to be 0.1 for cones (against p = 1 for rods). For completeness' sake we add that, since η rapidly decreases within the pupillar aperture by the Stiles-Crawford effect proper, we approximately have for the large natural pupil: $\eta_{\text{cones}} \approx \frac{1}{2}$.

7.3 The scattering mechanism of the retina

The retina exists of numerous larger and smaller structures, which together form the nervous network. They are embedded in normal tissue fluids (Fig. 7.3.1). Data on size, number and refractive index are scarce, but from Polyak's standard work (1948) we can understand that the largest elements are the ganglion cells, which measure about 10 μ in diamter, and the somewhat smaller nuclei in the inner and outer nuclear layers. Between and in them are numerous smaller structures. All these structures differ from their environment by their refractive index. Differences in absorption may be neglected in the visible part of the spectrum. They scatter, just because of these refractive jumps. It will be clear, that we have to schematize if we will come to a quantitative description of the scattering processes. We will base our computations on a scatter model of the retina, consisting of spherical particles, larger than 5 μ, with a refractive index m = 1.05 with respect to their surroundings (μ = m-1=0.05).

The following arguments may justify this rigorous simplification.[1] The scattering capacity is proportional to μ^2 for $\mu \ll 1$ and so, the structures with relatively large μ will certainly predominate. In view of what is a normal

[1] Much of our knowledge of scattering processes is taken from Van de Hulst's standard work (1957).

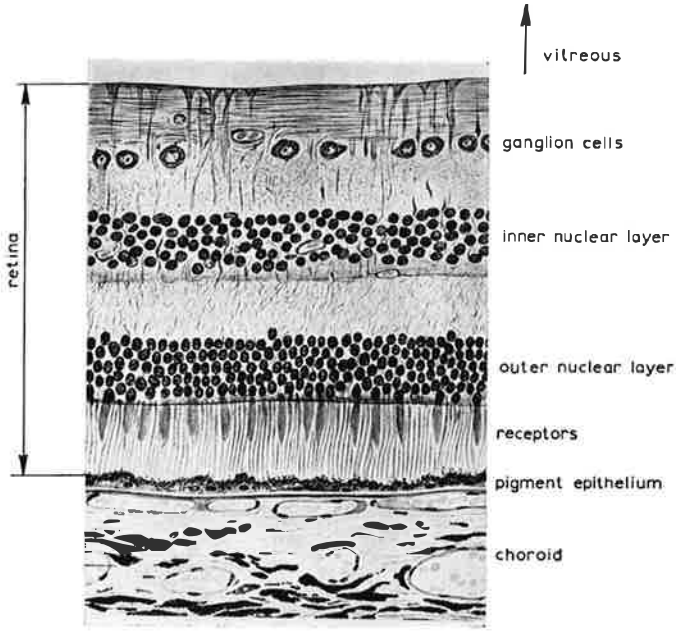

Fig. 7.3.1. Cross section through the peripheral retina and the adjacent layers (according to Bargmann 1962, with kind permission).

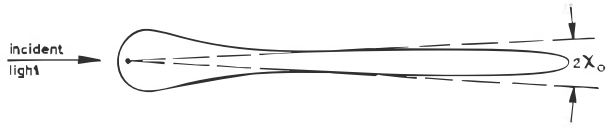

Fig. 7.3.2. The scatter diagram of the dominant retinal scattering particles.

spread in refractive index in this type of tissue, an effective value of m $\approx$ 1.05 sounds reasonable (Barer 1957). A diameter of 2 μ is a critical size for these particles (phase retardation $\sim$ 2 π rad). The scattering capacity is proportional to the square of the particle volume for diameters, small with respect to this size. Beyond this size, a saturation level is reached, in that sense, that the scatter capacity becomes proportional to the volume itself. In view of these data, it seems presumable that the larger sizes predominate.

The scatter diagram of these particles essentially consists of two parts (Fig. 7.3.2). In the non-forward directions, the laws of geometrical optics apply and the diagram is independent of the particle size. We have simply to apply Fresnel's reflexion formulas on a spherical surface under the simplification $\mu \ll 1$. The result can be summarized in the formula

$$\kappa_{1,2} = \frac{\mu^2 N}{8\pi} \cdot \frac{[\cos^2 \chi]}{(1 - \cos \chi)^2} = \sigma_{1,2}\, \mu^2 N. \qquad (1)$$

In this formula κ = fraction scattered per steradian; the suffix indicates the polarization component concerned.

N = number of scattering particles transmitted.

And χ = scatter angle = angle of incidence at the retina (§ 7.2).

The brackets indicate, that the term they include has to be used only for the component vibrating in the scatter plane (κ_2). The next table gives the values of $\sigma_{1,2}$ for four directions:

Table 7.3.3

The scatter indices $\sigma_{1,2}$ for various scatter directions χ

Scatter direction χ	σ_1	σ_2	Polarization for natural incident light
180° (straight backward)	0.040	0.040	0%
135° (obliquely backward)	0.055	0.028	33%
90° (sideward)	0.16	0.00	100%
45° (obliquely forward)	1.86	0.93	33%

The approximative expression for $\kappa_{1,2}$ loses its validity for $\chi < 45°$. Moreover, we approach then the forward scatter directions for which the laws of geometrical optics do not apply at all. In these directions the diffraction dominates. When we disregard interference details, one main central lobe stands out, which contains the lion's share of all scattered light. From Van de Hulst's Fig. 34 we read,

that this lobe has an effective aperture $2\,\chi_0 \sim 60\,\lambda/d$ (d = particle diameter for $\mu = 0.05$ (Fig. 7.3.2). Here χ_0 means that angle, within which 2/3 of all energy is scattered. We find $2\,\chi_0 = 6°$ for $\lambda = 0.5\,\mu$ and $d = 5\,\mu$. The energy within this lobe is distributed approximately according a Gauss-curve and that means that repeated — say N-fold — forward scattering, results in an effective aperture of the scattered beam of $\pm 3° \sqrt{N}$.

The above is valid under the condition that we deal with independent and single scattering. These conditions are not completely fullfilled.

Because of the small value of μ, multiple non-forward reflexions will hardly occur. Besides, the scattering particles are more or less spread at random, so that there is no systematic interaction and we may regard therefore their scattering as independent. The forward scattering, on the contrary, is neither single nor independent. The effective cross section—almost entirely due to a small forward lobe—measures about twice the geometrical cross section, which means a high scattering efficiency (multiplicity!) and also, that ample room is needed to develop the diffraction pattern. This now is hampered to some extent certainly by the proximity of other particles (Fig. 7.3.1), so that the tissue becomes more homogeneous as it were.

As a result, the 6° aperture must be considered as an upper limit. Moreover, we have to account for repeated forward scattering, eventually combined with one reflexion. The only effect of this multiple forward scattering on the sideward scatter pattern is some blurring of the details over $\pm 3° \sqrt{N}$, in which N denotes the number of particles to be passed. It can be estimated of the order of 10 from Fig. 7.3.1. Now there are no pregnant details at all according to (1). Since forward scattering is independent of the state of polarization, the sideward reflexion remains almost completely polarized. Finally we have made it plausible, that the scatter contribution of small particles can be neglected. This was derived from the integrated scattering cross section. Where the forward lobe gets more and more pronounced with increasing particle size, there is some chance that this neglection is not fully allowed for the non-forward directions. In this connection it is important to note that small particles too, give 100 % polarized straylight under 90°.

7.4 The retinal component

With help of the assumptions of §§ 7.2 and 3, we can now estimate

the straylight distribution over the fundus, due to retinal scattering. Using the notation of Fig. 7.1.1, we find:

$$\varepsilon_x = \int_0^L \phi\,\beta\,dl \quad . \quad f_\chi \quad . \quad 1/s^2 \quad . \quad \eta_\chi \qquad (1)$$

fraction of ø scattered in dl | fraction of it per sr round χ | solid angle of unit area | efficiency of excitation

ε denotes the "luminous effect" (§ 7.2) which here takes the place of the retinal illumination in view of the special receptive structure of the retina. This formula can be reduced to:

$$\varepsilon_x = \frac{\phi\,\beta}{x} \int_L f_\chi\,\eta_\chi\,d\chi\,. \qquad (2)$$

In order to compute the equivalent veiling brightness B_{eq}, we determine ε for normally incident light as well:

$$\varepsilon_{eq} = B_{eq} \cdot \underbrace{\frac{\pi\,D_v^2}{4\,F^2}}_{\text{solid angle of incidence}} \cdot \eta_v \qquad (3)$$

in which the index "v" points to the "equivalent veil" condition ($\eta_v = \eta_{pupil}$ in natural perceptive circumstances or $\eta_v = 1$ for experiments with a small entrance pupil). The meaning of D, F and other

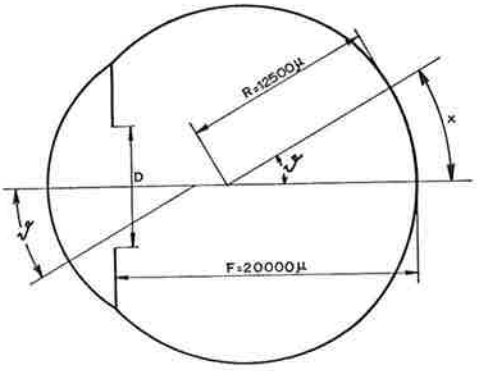

Fig. 7.4.1. Simplified geometrical optics of the human eye.

symbols can be read from Fig. 7.4.1, which represents a schematic eye. Equalizing ε_x to ε_{eq} and substituting $\phi = \pi/4\ D_g^2\ E_g$ (g points to the glare situation), we get:

$$B_{eq} = \frac{D_g^2}{D_v^2} \frac{F^2 \beta}{x \eta_v} E_g \int_L f_\chi \eta_\chi \, d\chi \,. \qquad (4)$$

Now $\beta f_\chi L$, the fraction scattered per solid angle, is equal to the formerly (7.3.(1)) derived expression $\sigma \mu^2 N$. We further assume that the experiments are carried out with small entrance pupils (so that $D_g = D_v$ and $\frac{\eta_\chi}{\eta_v} = p$). Then we have:

$$B_{eq} = \frac{F^2 \mu^2 N p E_g}{L x} \cdot \int_{\tan \chi = x/L}^{\infty} \sigma \, d\chi \qquad (5)$$

For not very small angles of glare ϑ we can further simplify because $x \gg L$. Then $\sigma \approx \sigma_{90^\circ}$ and $\triangle\chi = L/x$. This, together with

$$\vartheta_{degrees} = 180/\pi \,.\, F/R \,.\, x/F = 90\, x/F \text{ (Fig. 7.4.1)} \qquad (6)$$

gives:
$$B_{eq} = 5 \,.\, 10^3 \, \mu^2 N \, \sigma_{90^0} E_g/\vartheta^2, \qquad (7)$$

which in essence is nothing but the well-known photometric law, that the intensity falls quadratically with increasing distance to the light source. Substitution of $\mu = 0.05$ and $\sigma_{90^0} = 0.08$ (for unpolarized light $\bar{\sigma} = \frac{\sigma_1 + \sigma_2}{2}$, compare Table 7.3.3), finally gives:

$$(B_{eq})_{retina} = p \, N \, E_g/\vartheta^2 \qquad (8)$$

The choice of p and N depends on the circumstances: whether we consider foveal blinding (glare source focused on the fovea; we count at Polyak's $N \approx 2$) or peripheral blinding (we count $N \approx 15$) and whether we deal with scotopic or photopic vision ($p = 1$ or 0.1; see § 7.2).

In foveal blinding, at low levels of glare:

$$p = 1,\ N = 2,\ B_{eq} = 2\, E/\vartheta^2$$

In foveal blinding, at high glare levels:

$$p = 0.1,\ N = 2,\ B_{eq} = 0.2\, E/\vartheta^2.$$

In peripheral blinding with foveal perception:

$$p = 0.1,\ N = 15,\ B_{eq} = 1.5\, E/\vartheta^2.$$

When x is not large with respect to L, we have to evaluate the integral (5) numerically with 7.3.(1). The results of these computations can be found in Fig. 7.4.2, where we plotted — among other, later on calculated contributions — the course of $(C/p)_{ret}$ as a func-

tion of ϑ. We remind: C = blinding capacity = B_{eq} / E, see 2.1.(1). Two curves are drawn: one for N = 2, L = 40 μ (foveal blinding) and one for N = 15, L = 300 μ (peripheral blinding). Both curves exist of a steep part ($\sim \vartheta^{-3}$ approximately) for small angles of glare and a more slowly falling branch ($\sim \vartheta^{-2}$) for large angles. They only differ as to their absolute level and the point of transition. The course of the polarization degree is represented as dotted lines at the bottom of the figure. For small angles of glare ($\chi < 45°$) computations begin to be difficult since the $(1 - \cos \chi)^2$ approximation for the denominator

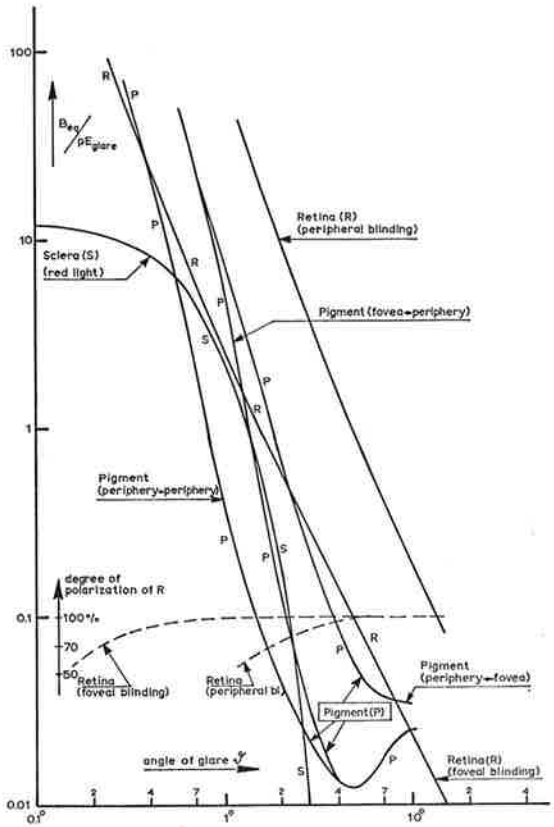

Fig. 7.4.2. The contribution of the various fundus components to the entoptic veil as a function of the glare angle ϑ. The absolute height of the curves is dependent yet on p, the value of the directional insensitivity of the photo receptors for strikingly incident light. In cone vision p = 0.1, in rod vision p = 1. Two curves are given for the retina (R) and even three for the pigment sheet (P). They differ, because of variations in thickness of the retina and in length of the outer segments of the receptors.

of 7.3.(1) begins to fail. Moreover we approach the forwardly directed diffraction lobes, for which the geometric optical approach does not hold at all. For very small angles, we have some hold at least to what is derived in § 7.2, namely that the intensity in the central lobe has a more or less Gaussian distribution with $\chi_0 = \pm 3°$ per scattering process. To determine the effective radius x_{eff} (Fig. 7.1.1) of this lobe, we use the well-known law of quadratic summation, valid for Gaussian distributions:

$$x_{eff}^2 = \sum_i x_i^2 = \chi_0^2 \sum_i 1_i^2 = \chi_0^2 \; N\,\overline{1^2} = 1/3\,\chi_0^2\,N\,L^2 \qquad \text{or}$$

$$\vartheta_{eff} = \frac{x_{eff}}{2R} = \frac{\chi_0\,L\sqrt{N}}{F\sqrt{3}};$$

with $\chi_0 = 3°$ per scatter process and $F = 20000\ \mu$:

ϑ_0 = diameter of the blur disc in minutes of arc $= 6\ 10^{-3}\ L \sqrt{N}$. (9)

For peripheral blinding: $L \approx 250\ \mu$, $N \approx 15$, so $\vartheta_0 \approx 6'$.
For central blinding: $L \approx 50\ \mu$, $N \approx 2$, so $\vartheta_0 \approx 0.4'$.

Of course these figures give only an order of magnitude. Anyhow, they show a remarkable influence of the foveal depression on the diameter of the blur disc.

7.5 The ophthalmoscopic fundus image

Our most important source of knowledge of the scleral and the pigment reflexion is the ophthalmoscopic image of the fundus oculi (see frontispiece). It is thought to be brought about in the following way (Fig. 7.1.1). The incident beam reaches the pigment layer, where it is partly reflected, and transmitted for the remaining part. This transmitted part passes the choroid and takes here the reddish color of the transmitted blood. Finally it reaches the whitish sclera, which reflects it to a considerable part. This reflected light again transmits the choroid and the pigment layer and finally it reaches the receptor layer again, where it produces false excitations.

This qualitative picture can be further worked out in a quantitative way with Brindley and Willmer's data (1952) about the spectral reflexion of the human fundus. As far as we know no other data are published.[1] We reproduce them in Fig. 7.5.1a, both for the periphery and for the macular region.

[1] After we had finished this chapter, we received Campbell and Alpern's data (1962). See § 8.3.

These results are not corrected for intra-ocular absorption and therefore we gathered the available data on ocular transmission (Fig. 7.5.1b). Since Brindley and Willmer's data were obtained after to and fro passage of the ocular media, we squared the original data of Geeraets e.a. (curve 3) and of Ludvigh and Mac Carthy (curve 1), which were measured at human eyes. Those measured at bovine eyes (curves 2 and 6) did not need squaring, because these eyes measure about twice the human eye in diameter. The rabbit data, on the other

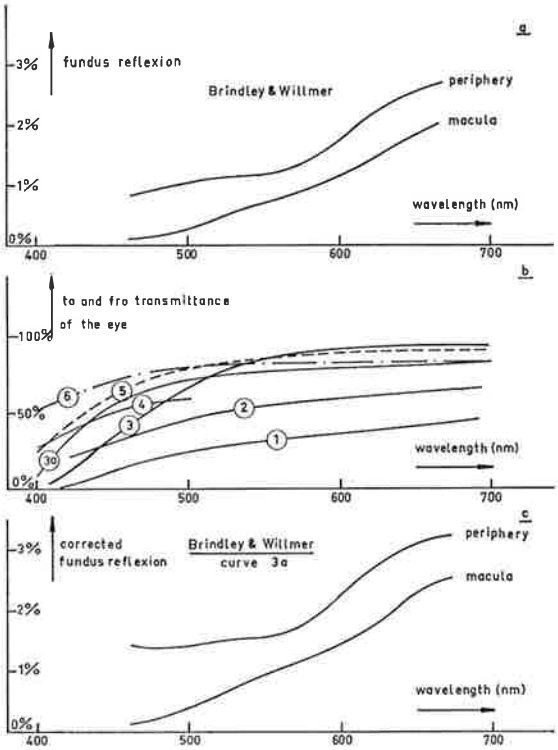

Fig. 7.5.1. The spectral fundus reflexion according to Brindley and Willmer (a) and its corrected course (c) on the ground of data on ocular transmission (b). (1) Ludvigh and MacCarthy (1938), [human eye][2]; (2) Roggenbau and Wetthauer (1927), [bovine eye][1]; (3) Geeraets e.a. (1960), [human eye][2]; (3a) ditto, [rabbit eye][3]; (4) Kinsey (1948), [rabbit eye][3]; (5) Wiesinger e.a. (1956), [rabbit eye][3]; (6) Pitts (1959), [bovine eye][1].

hand, (curves 3a, 4 and 5), are raised to the third power for similar reasons. The curves agree qua general trend but notably differ in accurate form and general level. The more recently published curves lie

much higher, presumably because of improvements in the always delicate technique of conservation. Attributing more weight to these recent curves, we chose curve 3a as "working curve" to determine the corrected fundus reflexion (Fig. 7.5.1c). In this figure we thus find two reflexion curves: one for the periphery, more or less flat with a clear rise in the red region; and one for the macula, which is notably depressed at the blue side of the spectrum. It is said, that the difference is due to the yellow macular pigment.

Now we have seen that the peripheral reflexion curve is composed of two parts: the pigment reflexion and the blood-colored scleral reflexion. The pigment seems to be more or less untinted black (melanine), so that its spectral reflexion curve must be flat. The scleral reflexion has to transmit some 300 μ sanguineous tissue (the choroid) which is thick enough, that only the red part of the visible spectrum is notably transmitted. It therefore sounds reasonable, to split the peripheral reflexion curve in a 1.5 % contribution of the pigment layer for all wavelengths and an extra 1.5 % contribution in the red region, due to the scleral reflexion.

We disregarded in the foregoing the influence of back scattering in the retinal tissue. On the ground of the theoretical speculations of § 7.3, the retinal remission in the backward direction amounts:

$$\kappa = \sigma \mu^2 N = 0.04 \times 0.05^2 \times 15 = 1.5\ 10^{-3} / \text{sr}$$

against a total fundus backward reflexion

$\kappa_{red} = 3\ \% / \pi = 10^{-2} / \text{sr};$ $\kappa_{green\ blue} = 1.5\ \% / \pi = 5\ 10^{-3} / \text{sr}.$

According to these theoretical considerations, the retinal remission is small with respect to the total fundus reflexion in the red part of the spectrum, but it cannot completely be neglected in the green/blue region. In this connection it is interesting to note, that Vogt (1921) proved that the retinal structures, which are invisible in normal ophthalmoscopy, just may appear in a red-free illumination of the fundus!

7.6 The pigment reflexion

In order to compute the course of the pigment component with the angle of glare, we have to consider a few complicating factors.

a. At scatter angles near 90° a granular surface like the pigment coat, does not obey Lambert's law. In Fig. 7.6.1 the grains — for clearness' sake indicated as "pickets" — obstruct the view on the illuminated pigment coat as it is seen from the "scatter direction".

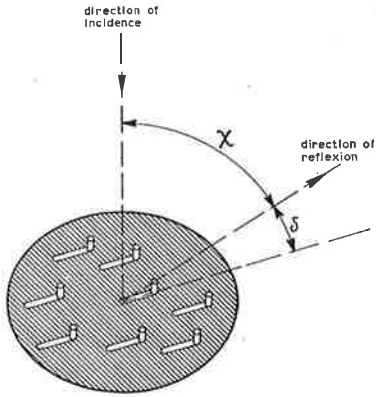

Fig. 7.6.1. Schematical representation of the granular appearance of the pigment sheet. The grains are indicated as pickets for clearness' sake. The white parts in the plane of the pigment sheet give no contribution to the reflexion in the indicated direction, as they are screened by the pickets.

For a quantitative description we introduce the *granularity* g = the total apparent surface of the grains in side view per unit of area. For round grains, this means the fraction of the total area, covered with grains. Now, the apparent reduction of the reflecting area with increasing angle χ does not obey Lambert's law ($\sim \cos \chi$), but occurs according to

$$(1 - g)\ (1 - g \tan \chi) \cos \chi + g \cos \chi\ . \qquad (1)$$

$g \tan \chi$ represents the fraction of the illuminated area, indicated without shading in Fig. 7.6.1 and $\cos \chi$ the normal perspective shortening. For simplicity we assumed that the granular structure is regular, so that the obstructed areas do not notably overlap before the whole area is obstructed; and that there are many small grains per unit of area, so that the area becomes almost completely unshaded (in Fig. 7.6.1) at last and a negligible fraction falls outside the illuminated area.

Now usually $\pi/2 - \chi = \delta \ll 1$, so

$$\varrho_\chi = \varrho_{pgm}/\pi \cdot \{(\delta - g)\ (1 - g) + \delta g\}\ . \qquad (2)$$

The factor π gets into this formula, because ρ_{pgm} was derived by Brindley and Willmer from ρ_{180° (the backward component) by applicating Lambert's law. The formula clearly exists of two parts.

$$(\rho_\chi)_1 = \frac{\varrho_{pgm}}{\pi}(\delta\text{-}g)\ (1\text{-}g) \approx \frac{\varrho_{pgm}}{\pi}\ (\delta\text{-}g) \text{ for } g \ll 1, \qquad (3)$$

which becomes zero for $\delta \leqslant g$ (the negativity for $\delta < g$ has no physical significance of course); and

$$(\rho\chi)_2 = \frac{\varrho_{pgm}}{\pi}\ \delta\ g \qquad (4)$$

which is the contribution of the top surface of the grains, obeying Lambert's law.

Now $(\rho\chi)_2 = [(\rho\chi)_1$ for $g = 0] \times g$. We will first determine therefore $(\rho\chi)_1$ and then compute.

$$(\varrho\chi)^{g=g_1} = (\varrho\chi)_1^{g=g_1} + (\varrho\chi)_1^{g=o} \times g_1 \qquad (5)$$

b. We recognize the importance of an accurate knowledge of δ as a function of the angle of glare. In the neighborhood of $\delta = g$, a small change in δ will have large consequences for $\varrho\chi$. Therefore, we have to account for the curved course of the fundus (Fig. 7.6.2).

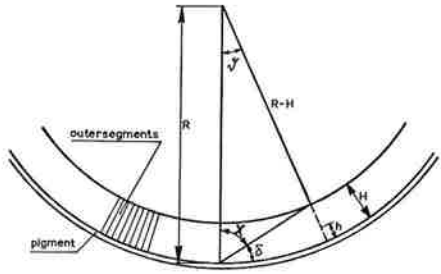

Fig. 7.6.2. Geometry of the optics of the pigment reflexion in relation to the curvature of the fundus.

Be R the curvature radius of the central fundus and H the length of the outer segments, then we get, by applicating the sine rule:

$$\frac{\sin\chi}{R\text{-}H} = \frac{\sin(\chi+\theta)}{R}, \text{ or, after some conversions: } \operatorname{tg}\delta = \frac{R/(R\text{-}H) - \cos\theta}{\sin\theta}$$

Usually $\delta \ll 1$, $\theta \ll 1$ and $H \ll R$ so that

$$\delta = \frac{H/R}{\theta} + \frac{\theta}{2} \qquad (6)$$

We combine (6) and (3):

$$(\varrho\chi)_1 = \frac{\varrho_{pgm}}{\pi}\left\{\frac{H/R}{\theta} + \frac{\theta}{2} - g\right\} \qquad (7)$$

Assuming that the retina is photo-sensitive over the whole length of the outer segments, we have to change this formula, replacing H by h (Fig. 7.6.2) and averaging over h:

$$\overline{(\varrho\chi)_1} = \frac{\varrho_{pgm}}{\pi H}\int\left\{\frac{h/R}{\theta} + \frac{\theta}{2} - g\right\} dh. \qquad (8)$$

The integration domain is determined by the demands that 1) the integrand cannot be negative:

$\frac{h/R}{\theta}+\frac{\theta}{2}-g \geqslant 0$, or $h \geqslant (g - \theta/2)\, R\, \theta$, and 2) $H \geqslant h \geqslant 0$.

This means, that we have to integrate from $h = (g - \theta/2)\, R\, \theta$ to H unless $\theta \geqslant 2g$. In that case we must integrate from 0 to H. As a result:

$$\overline{(\varrho\chi)}_1 = \frac{\varrho_{pgm}}{\pi}\left[\left\{\frac{H}{2R}\,\frac{1}{\vartheta} - g + \frac{\theta}{2}\right\} + \frac{R\,\theta}{2H}\left\{g - \theta/2\right\}^2\right] \qquad (9)$$

to be cancelled for $\theta > 2g$.

Accounting for all mentioned pecularities of the receptive and reflective mechanisms involved, we arrive at:

$$\overline{\varrho_\chi} = \frac{\varrho_{pgm}}{\pi}\left[\left\{\frac{H}{2R}\,\frac{1+g}{\vartheta} - g + \frac{(1+g)\,\vartheta}{2}\right\} + \frac{R\,\vartheta}{2H}\left\{g - \vartheta/2\right\}^2\right] \qquad (10)$$

to be cancelled for $\vartheta > 2g$

Now matters become relatively simple: Using the formerly introduced ε-terminology, we have (Fig. 7.1.1):

$$\varepsilon_x = \overline{\varrho_\chi} \cdot \frac{\phi}{s^2}\,\eta_\chi \qquad (11)$$

and, by proceeding along the already paved ways of § 7.4, we arrive at:

$$B_{eq} = \left(\frac{\eta_\chi}{\eta_v}\right)\cdot\left(\frac{D_g}{D_v}\right)\frac{\overline{\varrho_\chi}}{s^2}\,R^2\,E_g \qquad (12)$$

The pigment reflexion can be assumed to be completely depolarized, so that only one half of it is subject to the polarized receptive mechanism, described in § 7.2: $\eta_\chi = \eta_v \cdot (\frac{1}{2} + \frac{1}{2}\cos^2\chi)$. p. We silently assumed here at the same time, that an artificial pupil was used, so that we also can take $D_g = D_v$. Finally $s/R = \vartheta$, so that:

$$B_{eq} = \frac{p}{2}(1 + \cos^2\chi)\,\frac{\overline{\varrho_\chi}}{\vartheta^2}\,E_g. \qquad (13)$$

Almost directly, the term in parentheses reduces to 1 (for $\vartheta > 20'$). Substituting further the expression for ϱ_χ, we get (ϑ in radians):

$$\frac{B_{eq}}{p\,E_g} = \frac{\varrho_{pgm}}{2\pi}\left[\frac{H}{2R}\,\frac{1+g}{\vartheta^3} - \frac{g}{\vartheta^2} + \frac{1+g}{2\,\vartheta}\,\frac{R\,\vartheta}{2H}\,(g - \vartheta/2)^2\right] \qquad (14)$$

to be cancelled for $\vartheta > 2g$

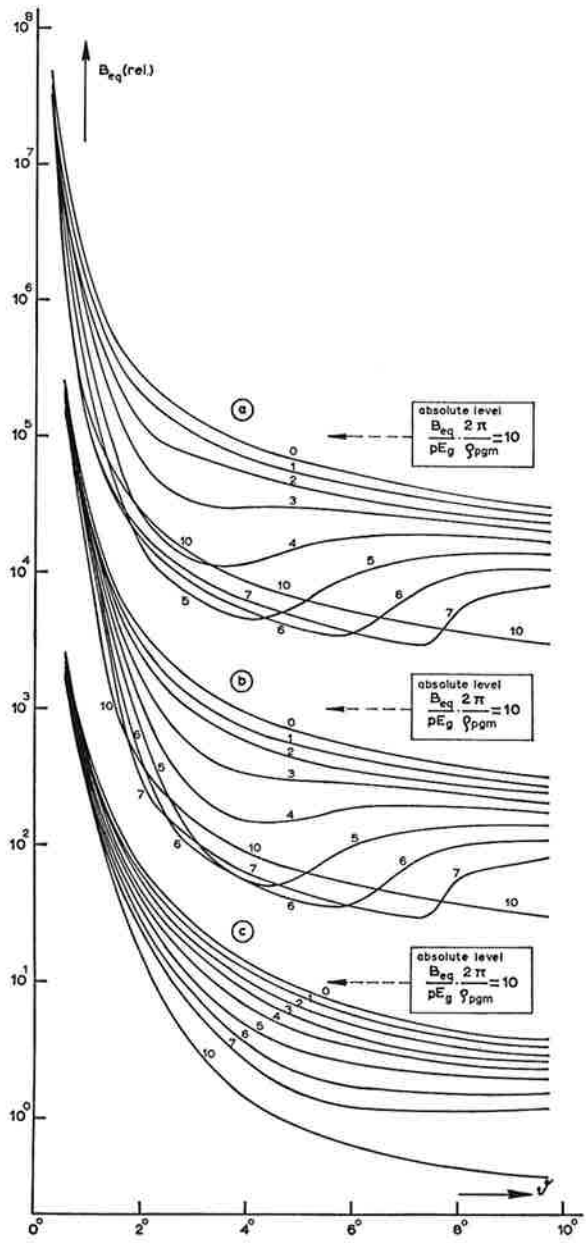

Fig. 7.6.3. The contribution of the fundus reflexion to the entoptic veil. a. Peripheral blinding, peripheral perception. b. Foveal blinding, peripheral perception. c. Peripheral blinding, foveal perception. The parameter is the granularity g, indicated in %.

In order to evaluate this expression, we have to substitute numerical values: $\varrho_{pgm} = 0.015$ (Brindley and Willmer), R = 12500 μ (anatomical datum). H depends on the eccentricity of the place of reception at the retina. Making a smooth course of Polyak's data (as tabulated by Le Grand, 1948), we assume H = 60 μ at the fovea, 40 μ at 0.02 rad eccentricity, 25 μ at 0.04, 20 μ at 0.06 and 15 μ beyond 0.07 rad. These data are given for cones only, but, guided by Polyak's illustrations, we assumed the same figures for the effective length of the rods for light, incident along the retina. In Fig. 7.6.3 we present the numerical results for a number of values of g (indicated as a parameter in %-values) and for three glare situations:

— foveal blinding, extrafoveal perception (situation Ch. II, H = H (ϑ)).

— peripheral blinding, foveal perception (situation § 4.4 and Ch. V, H = 60 μ).

— peripheral blinding, peripheral perception (situation Ch. III, H = 15 μ).

We note a strong influence of the granularity in the critical range where the distance to the retinal image of the glare source is large enough to get χ near 90°, but yet small enough to have no "profit" of the curvature of the fundus.

The dip is very deep in the last case (*a* in the figure), where H is small (the outer segments almost completely vanish in the grain shadows) and is almost absent for the long foveal receptors (*c* in the figure). In the next chapter, we will have to make a choice, which value of g makes the best fit with the experimental results. Anticipating, we already drew in Fig. 7.4.3 the curve for g = 0.06 $\pm$ 0.01 (that is: the average curve over g = 0.05, 0.06 and 0.07).

7.7 The scleral reflexion

Again we will use the notation of Fig. 7.1.1, now for the downside right part. The general train of thoughts is quite the same as in the former section. We have only to account now in addition for the absorption in the choroid and pigment layer, which of course increases with increasing value of χ. Therefore, we write:

$$\varrho_{app} = \tau^2 \varrho_{scl} , \qquad (1)$$

in which ϱ_{app} indicates the apparent scleral reflexion as it contributes to the ophthalmoscopic fundus image, right across the pigmented layers; ϱ_{scl} the reflexion factor of the sclerotic coat proper,

and τ the transmissivity of the pigmented layers in perpendicular transit. Substituting ϱ_{app} = 1.5 % (red) or zero (blue/green) and taking for ϱ_{scl} a 55 % value (measured at the visible part of the white of the eye), we find:

$$\tau = \sqrt{\frac{1.5\ \%}{55\ \%}} = 16\ \%\ \text{(red) or zero (blue/green)}.$$

The absence of a blue transmission peak in Fig. 7.5.1 — like haemoglobine has — indicates, that the thickness of the blood layer is more than 250 μ, which seems to be a high but not impossible value for a double passage through the choroid.

We go now the same way as in § 7.6, with this difference, that we are allowed here to neglect the curvature of the fundus. We find:

$$B_{eq} = 2.3\ \ 10^5 \cdot \left(\frac{\eta_\chi}{\eta_v}\right) \cdot \left(\frac{D_g}{D_v}\right) \varrho_{scl}\ \frac{T}{F}\ \sin^3\chi \cdot \tau^{\,1\,+\,{}^1/\cos\chi}\ \frac{E_g}{\vartheta^3_{degrees}} \qquad (2)$$

In this formula, the third power of ϑ is produced by the combined influence of the fall of the intensity with increasing distance along the retina ($\sim {}^1/\vartheta^2$) and the apparent shortening of the scatter source ($\sim {}^1/\vartheta$). By substitution of $D_g = D_v$, the η-expression, ϱ_{scl} = 55 %, τ = 16 %, T = 300 μ and F = 20000 μ, we arrive at:

$$B_{eq} = 150 \times 0.16^{\,{}^1/\cos\chi}\ \sin^3\chi\ (1 + \cos^2\chi)\ p\ \frac{E_g}{\vartheta^3_{degrees}} \qquad (3)$$

The full course of the $(B/pE)_{scl}$ relation is drawn in Fig. 7.4.3 with other B/pE curves. It shows a flat course for $\vartheta \ll 1°$ ($x \ll T$) and a steep fall, when the combined influence is felt of absorption, distance and perspective shortening.

7.8 The corneal reflexion of the fundus image

The aim proper of this chapter was to study the fundus to fundus remission. However, our computations above permit us to determine by the way the brightness of the corneal reflexion of the fundus image (Fig. 7.8.1):

$$\varepsilon = E_g \frac{\pi D^2}{4} \cdot \frac{\varrho_f}{\pi} \cdot \left(\frac{3.8}{23}\right)^2 \cdot \left(\frac{m-1}{m+1}\right)^2 \cdot \frac{1}{F^2} \cdot \tau^2 \qquad (1$$

not much dependent on x	incident flux	backward reflexion	ω_1/ω_2	corneal reflectivity	sr/m²	double trans-mittance

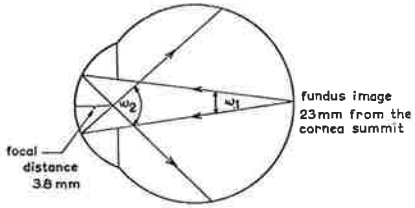

Fig. 7.8.1. The geometry of the corneal reflexion of the fundus image.

This, together with formula 7.4.(3) gives:

$$B_{eq} = \frac{\varrho_f \cdot \tau^2}{\pi} \cdot \left(\frac{D_g}{D_v}\right)^2 \cdot \frac{1}{\eta_v} \left(\frac{3.8}{23}\right)^2 \cdot \left(\frac{m-1}{m+1}\right)^2 \cdot E_g \qquad (2)$$

or, with $m = 1.34$, $D_g = D_v$, $\eta_v = 1$ (small entrance pupil) and $\varrho_f \tau^2 = \varrho_{app\ fundus} = 1\ \%$ (Fig. 7.5.1a):

$$B_{eq} \approx 5\ 10^{-6}\ E_g\ . \qquad (3)$$

It is evident, that this contribution is negligible all over the retina in comparison with the other contributions.

7.9 Comparison with other investigators

Not many investigators have paid attention to the problem of fundus remission. Only four of these few have tried to come to a more quantitative evaluation along theoretical ways. It is worth while to compare their and our results.

Borschke (1904) considered the fundus as an integrating sphere and expected a uniform veiling brightness all over the fundus therefore. Since he found a rapid fall of the veil brightness with increasing glare angle in his experiments he abandoned this point of view. Recently, Brindley and Willmer (1952), in their previously mentioned paper, made more or less the same fault of making a rough estimation on the ground of an over-simplified model. The quintessence is, that the receptor layer is not a smooth, geometrically thin and optically dense surface.

Pokrowski (1926) assumed, that the blood vessels in front of the retina were responsible for the straylight. From this starting point he could derive the $1/\vartheta^2$ law for large angles. For smaller angles, his method failed, because he assumed isotropic scattering in stead of a strongly forwardly directed scatter pattern. A more important difference with our results: he could not compute the absolute level of the equivalent brightness. Le Grand (1937) indicated some minor and not clearly motivated changes only in Pokrowski's final formula.

He also mentions the corneal reflexion of the fundus image, but comes to an about hundred times larger effect than we computed, though he assumed a corneal reflexion of only 2 %. Our assumption was:

$$\left[(1.34 - 1) \;/\; (1.34 + 1)\right]^2 = 6\ \%.$$

The origin of the divergence could not be found out.

Concluding, we can only say, that the harvest in the domain of theoretical investigations on fundus straylight is extremely scanty and almost useless in our proceeding.

7.10 Review

In this chapter, we discerned three types of fundus straylight: retinal straylight, the pigment reflexion and the scleral reflexion. We omit here the corneal reflexion of the fundus image (§ 7.8), which turned out to be negligible. The behavior of these three types as a function of the angle of glare ϑ (in retinal terms: as a function of the distance along the retina) can be read from Fig. 7.4.3. We once again take through — in broad outline — its composition.

If we had not known anything about the scattering and receptive mechanisms involved, we should have expected, with Borschke, an homogeneous light distribution all over the field of view. The bulbus would act as an integrating sphere. The following corrections on this view had to be applicated:

a. The visual pigment forms no optically dense absorptive layer. The retina is almost transparent, its excitability does not depend on the angle of incidence and a fall of $B_{eq} \sim {}^1/\vartheta$ is introduced.

b. Moreover, the cone receptors are preferentially sensitive for normally incident light (the Stiles-Crafword effect) and thus relatively insensitive to fundus straylight. The factor p in the ordinate expression of Fig. 7.4.3 accounts for this effect.

c. The retina is transparent as well as a scattering medium. This introduced another factor ${}^1/\vartheta$ in the expression for B_{eq}. Together with the effect sub *a*, it makes that $B_{eq} \sim {}^1/\vartheta^2$. Deviations for small angles are due to the forwardly directed scatter pattern of the retinal tissue and its finite thickness.

d. The retina has not the same thickness over its full surface. At the place of the fovea, it is notably thinner and this results in a marked depression in the amount of straylight of retinal origin. Therefore, two curves are drawn, one for foveal and one for parafoveal blinding.

e. The pigment layer is not a transparent reflectans and thus, one should expect a $^1/\vartheta$ dependence. In fact, this relation holds for large angles of glare, say beyond 20°. For smaller distances, two effects occur: First, the $^1/\vartheta^2$ course is not mitigated any longer by the perspective shortening of the scatter center because of the finite height of the receptive layer. On the contrary, it reaches a maximum for $\vartheta = 0$ and, as a result the pigment reflexion has a steep course $\sim {}^1/\vartheta^3$ at small angles. Second, the granularity of the pigment coat makes, that there is an effect of self-screening. It is small for small angles of glare, because the height of the outer segments is large with respect to the grain size. And it is small for large angles of glare, because the curvature of the fundus raises the outer segments out of the screening zone. In the intermediate range, round about 5° glare angle, it gives a reduction of the pigment component, which takes the shape of a deep dip in the case that the outer segments are short (in peripheral perception).

f. The scleral contribution too, does not reach the $^1/\vartheta$ course within the domain studied here, because of two other effects. First, the oblique passage of the reflected rays through the pigment coat gives an almost complete suppression already beyond 3°. And second, the thickness of the interjacent choroid (300 μ) gives a saturation level for retinal distances, small with respect to this value (for $\vartheta \ll 1°$).

In comparing the various curves, we notice that, in peripheral blinding, the retina takes a dominant place. In foveal blinding it is the most important component yet, but it is comparible in size then with the pigment reflexion. For large angles, beyond 20°, the pigment reflexion will even take the lead. The scleral component very soon becomes unimportant because of the large absorption in the pigmented layers in oblique transit. It will show some kind of come back like the pigment reflexion, due to the spherical form of the bulbus, but only for very large angles at regions of the retina near the ora serrata. The red appearance of the fundus will be observed therefore only in backward reflexion. As a consequence, the polarization degree of the fundus component is almost 100 % in peripheral blinding, wheras it will fluctuate round the 70 % in foveal blinding (for $\vartheta < 15°$). Unnecessary to say, that in particular the absolute height of the various curves is strongly dependent on the assumptions made. Therefore, these polarization data may be subject to notable change when we change the underlying assumptions.

CHAPTER VIII

STRIKING THE BALANCE

8.1 Review of our approach

In the first part of this thesis, we showed the absence of neural effects in glare in the situation we studied it (Ch. II and III), and we got an indication of the importance of fundus straylight from the inflexion in the equivalent veil curves (§ 2.3). Therefore, we concentrated from then upon how the various media — and in particular the fundus — contribute to the scatter veil on the retina. We investigated the Boehm brushes (Ch. IV), which informed us about the share of the retina itself. We measured the Stiles-Crawford effect for the scatter veil (Ch. V), which allowed us to weigh the contributions of the cornea and lens against that of the fundus — that is: retina, pigment layer and sclera together. And finally, the method of iris shadow casting (Ch. VI) gave us a rough impression of the corneal share at large angles of glare. Each of these approaches strengthened us in our conviction, that the fundus must play an important role in fact. Therefore, we devoted a special chapter (Ch. VII) to a theoretical analysis of the fundus remission.

Now, having come to the end, we must strike the balance. We must weigh the various experimental results, judge them in the light of the theoretical speculations mentioned, and finally try to fit them — if possible — in one general concept of a mechanism of glare. However, before we can start, we will have to pay some attention yet at what we know about the behavior of other types of entoptic straylight: from the cornea, from the crystalline lens and from the vitreous humor.

8.2 Other types of straylight

Objective experimental data on entoptic straylight in the range of glare angles we studied, do not exist. The data, obtained by Boynton and co-workers (Boynton, Enoch and Bush 1954; DeMott and Boynton 1958) only relate to larger scatter angles and Flamant (1955), DeMott (1959), Westheimer and Campbell (1962) and Krauskopf

(1962) worked only at angles in the order of minutes of arc. Computations are difficult, since the cornea and lens, the principal sources of straylight in the slit lamp image (frontispiece), contain quite heterogeneous and not always spherical scatter substances. Therefore, extra-polation of the existing scatter data must be thought a precarious business. The vitreous is definitely less cloudy than the cornea and lens on the slit lamp image. It is about four times thicker than the lens, however, and more close to the retina besides. Therefore we cannot eliminate *a priori* its influence, but it seems presumable that we are allowed to split up schematically the vitreous into two parts: an anterior part, which acts together with and undiscernably from the cornea and lens; and a posterior part, which more or less acts as a part of the fundus.

8.3 Splitting up the entoptic veil in constituent parts

We have some freedom yet in the appropriate choice of the cornea and lens constituents, since we do not know much of them. But as to the fundus components, we are more or less bound by the theoretical analysis of the former chapter. More or less, as the accuracy of the absolute heights is not great and the course with ϑ of the pigment component is dependent on the particular assumptions on its granularity g. It seems best to us, that we do not bother the reader with the whole process of trial and error to attain a satisfactory split up, but that we walk the inverse way. We will at once present the final result of all considerations and after it, we will explain its construction, argument our assumptions and discuss its significance.

Table 8.3.1

Best fitting split up of B_{eq}/E in sr^{-1} over the various media for two glare angles

Angle of glare	Glare scene	Cornea and lens	Retina	Pigment layer	Sclera	Fundus as a whole	All components
1°	py→fv	20	7	6	1.3	14.3	34.3
	fv→sc	20	2.6	40	13.4	56	76
	fv→ph	20	0.3	4	1.3	5.6	25.6
	py→ph	20	7	0.3	1.3	8.6	28.6
4°	py→fv	0.60	0.15	0.07	—	0.22	0.82
	fv→sc	0.60	0.15	0.10	—	0.25	0.85
	fv→ph	0.60	0.015	0.010	—	0.025	0.63
	py→sc	0.60	1.5	0.10	—	1.60	2.20

Notation: py = periphery, fv = fovea, sc = periphery at scotopic level, ph = ditto at photopic level, A → B = glare source focused at A, perception with B.

The values of the retina column are read from Fig. 7.4.3, on that understanding, that the appropriate value of the Stiles-Crawford factor p (the directional insensitivity, 1 in rod vision and 0.1 in cone vision) is substituted according the perceptive situation. The choice of the pigment values was less simple. In the first place, we had to make an assumption about the granularity g. Anatomically, we have no other indication, than that the sheet is granular to some extent. We need the granularity as a parameter because the dip round 4° (Fig. 7.6.3 a and b) might account for the absence of the inflexion in the equivalent veil curves (Fig. 2.3.3) at angles beyond some 3°. The dip would produce a strong depression of the entoptic veil brightness at these angles. We finally chose g = 0.06 ± 0.01, because it gave a reasonable fit and because the set of curves (Fig. 7.6.3 a and b) shows a clear condensation round that value. Apart from this choice of g, we changed the pigment values in another way, in that we multiplied them by a factor 8. This was necessary to get the steep fall in the entoptic veil in the mesopic range (the dip can only explain it, if it plays a sufficiently dominant role). We found a justification for this manipulation in a private communication by Campbell and Alpern (meanwhile published 1962), that they, in repeating Brindley and Willmer's measurements, found some ten times higher values for the fundus reflexion factor. We can not judge at the moment the reliability of either of these data. Apparently our knowledge is rather defective and we felt justified in this situation to take some freedom as to the appropriate choice of the fundus reflexion. As a consequence, the scleral values of Fig. 7.4.3 have to be multiplied by a factor $8\frac{1}{2}\ (1 + 1/\cos\chi)$; which, for $\theta = 1°$ is a factor 6. The cornea and lens values, finally, have been chosen in such a way, that they gave the best fitting final results.

We now compare this split up with the experimental data:

a. The Boehm II experiments (§ 4.5, py → fv situation) gave some 21 % for the retinal share. We read in Table 8.3.1: 7 / 34.3 = 20 % at 1° and 0.15/0.82= = 18 % at 4°.

b. The Stiles-Crawford experiments (Ch. V, py→fv situation) gave about 30 % for the fundus share. We read here: 14.3 / 34.3 = 42 % at 1° and 0.22/0.82 = 27 % at 4°.

c. The equivalent veil experiments (Ch. II, fv→py situation) gave a fall in the veiling capacity over some factor 3 at 1° during the mesopic transit, but showed no inflexion at all at 4°. We read here:

$$\frac{\text{Total (fv}\rightarrow\text{sc)}}{\text{Total (fv}\rightarrow\text{ph)}} = \frac{7.6}{25.6} = 3.0 \text{ at } 1° \text{ and } 0.85 / 0.63 = 1.35 \text{ at } 4°.$$

d. The Boehm I experiments are performed in a less definite glare situation. The perception takes place over a wide field of view as an overall effect and we do not know exactly whether it is in scotopic or in photopic vision. Perhaps we best approximate the perceptuel conditions in taking an average between the following conditions:

Foveal effect		Parafoveal effect	
Experimental value $\approx$ 12%		Experimental value $\approx$ 40%	
fv→ph,	1° : 0.3 / 25.6 = 1%	py→fv,	4° : 0.15 / 0.82 = 18%
fv→sc,	4° : 0.15 / 0.85 = 18%	py→ph,	1° : 7 / 28.6 = 25%
		py→sc,	4° : 1.5 / 2.2 = 68%

e. In § 2.3 we found for the total entoptic veil $B_{eq} / E = 29 / \vartheta^{2.8}$, so that we can compare the theoretical and the experimental values: at 1° (fv→ph, see Fig. 2.3.3) $B_{eq} / E = 25.6$ (th.) against 29 (exp.), at 4° (fv→sc) $B_{eq} / E = 0.85$ (th.) against 0.60 (exp.).

f. The scleral component plays a minor role according to the Table 8.3.1, such in concordance with the experimental finding, that the wavelength is an insignificant parameter in glare phenomena.

g. The results of Ch. III and VI fall outside the range of ϑ-values over which we computed all fundus components. But we can extrapolate the curves of Fig. 7.4.3, without claiming much accuracy of course, because the approximations on which they are based are not valid beyond this range. For the iris shadow experiments we arrived at the following best fitting split up (at 20°):

Scene	Cornea	Lens	Retina	Pigment	Sclera	Fundus	All media
py→fv	0.01	0.004	0.005	0.016	—	0.021	0.035
fv→sc	0.01	0.004	0.007	0.16	—	0.17	0.18

The cornea component is taken from Fig. 6.3.1, the lens component using DeMott and Boynton's data (§ 6.1). The figure 0.035 for the total veil can be compared with the experimental value $B_{eq} / E = 10 / \vartheta^2 = 0.025$ (average result of the experiments, mentioned in Table 2.3.5), but we must bear in mind that these experiments are done with a natural pupil. In § 6.3, we compared the cornea component — about 0.3 cd/m² at 20° and for E =40 lux, so $(B_{eq}/E)_{cornea} \approx 0.01$ sr^{-1} — with this 0.025 figure, valid for the py→fv situation, and came to a corneal share of some 30 %. The analysis of Ch. VII has changed our view in so far, this this percentage only holds for the situation in which the fundus component is reduced by the use of the photopic receptive mechanism (in foveal perception e.g.). In the

situation, we investigated in Ch. VI, we presumably worked at scotopic levels at 20° and then we have to compare this 0.01 value with the 0.18 value, valid for the fv→sc situation. We conclude that in the iris shadow experiments, the corneal share might have been some 5 % only.

h. In the equivalent veil experiments of Ch. III we did not find a fall in the blinding capacity in the mesopic range. The absence of a fall can be explained, like we explained the absence in foveal blinding at large angles, by a sufficiently high level of the masking veil from the cornea and lens. This would mean that the cornea / lens contribution should be large with respect to 100 sr^{-1} (extra polated fundus value) at 0.5°. And this, in turn, would mean, that the joint contributions of cornea and lens should show a very sharp forward peak with an effective aperture of no more than 1°. That this is not impossible, might be indirectly derived from the fact that there is a clear correlation between the scatter capacity (measured in backward direction) of the cornea and lens and the visual acuity (Allen and Vos, in experiments on subjects between 6 and 86 years old). A more direct argument can be found in DeMott's measurements on excised eyes (1959). This can only be so, if at the small angles, relevant in visual acuity, the cornea and lens influence is comparable at least with the other straylight components. We might attribute such a strongly forwardly directed scatter diagram to the flat cellular structures of the cornea and lens epithelium.

The above is a trial to explain the phenomena observed within the concept of a pure straylight mechanism of glare. Its successes are not overwhelming, but many of the experimental results can yet roughly be understood along this way. The agreement is not great in details, but the order of magnitude is satisfactory most time and more can hardly be expected with such a necessarily rough theoretical description and with such "marginal" experiments as a base.

8.4 Conclusions

We survey now the main findings of this thesis:

a. The parallelism between the masking action of a glare source and of an ectoptic light veil is almost complete. No serious indications were found for the existence of a neural component in glare, in the way we defined and investigated it (Ch. II and III). The parallelism is most simply explained in terms of entoptic straylight.

b. The only clear deviation from a strict linearity in these experiments (Ch. II) is the exception which proves the rule. The reduction in blinding capacity at photopic brightness levels could be explained in terms of a directional insensitivity of the cone receptors in sideward directions (the complement of the Stiles-Crawford effect), if we assumed, that the fundus image of the glare source is an important source of entoptic straylight.

c. The other experiments confirmed this view. The brightness of the entoptic veil proved to be related to the physical stimulus condition (polarization, place of entrance at the pupil, screening by the iris) rather than to the glare intensity in physiological units.

d. The relative contributions of the various eye media to the glare veil depend on the angle of glare and on the further stimulus conditions, like the brightness level (scotopic or photopic vision) and the position of the glare source in the field of view (foveal or extrafoveal). Roughly we can state, however, that there are three main sources of straylight: the cornea, the lens and the fundus; and that they contribute with shares which, generally said, do not differ in order of magnitude. We definitely reject a model of a homogeneously diffusing bulbus (Stiles, 1930; Fry, 1954).

e. The veil brightness is almost independent of the wavelength of the glare light. This needs not to offer serious difficulties to a straylight explanation. There is no reason to expect a dominance of Rayleigh scattering in the eye (§ 7.3) and the red color of the fundus reflexion in ophthalmoscopy (backward remission) proved to be no measure of the color of the fundus component in glare phenomena (scattering round 90°, § 7.5).

f. In general we can say, that the glare mechanism of the fundus component is so complicated, that a detailed analysis only, can lead to useful results. Essential elements in such an analysis are:

— the transparency of the retina both as a scattering and as a receptive structure.

— the action of the pigment epithelium both as a reflectans and as an absorbens (anti-halation coat for the scleral reflexion).

— the depressive influence of the directional insensitivity of the cone receptors for other than perpendicularly incident light.

Quantitatively, we can represent the results of this thesis as an extended revision of Fig. 7.4.3. Fig. 8.4.1 gives the course of the various components of entoptic straylight, according the ideas developed in this thesis. We recognize, that it is not easy to read this

figure in a single glance. Without repeating the arguments of § 7.10, we may describe therefore the course of the various curves with a few words.

Two retinal curves are drawn: one for peripheral and one for foveal blinding. The difference is due to the foveal depression. They show a fall, quadratic for large angles, somewhat steeper for the smaller angles.

The pigment contribution is even represented by three curves. Their only difference lies in the assumption of the length of the outer segments of the receptive elements. The shorter the outer segments, the stronger the influence of self-screening by the pigment grains.

The scleral contribution has a clearly divergent course. For small

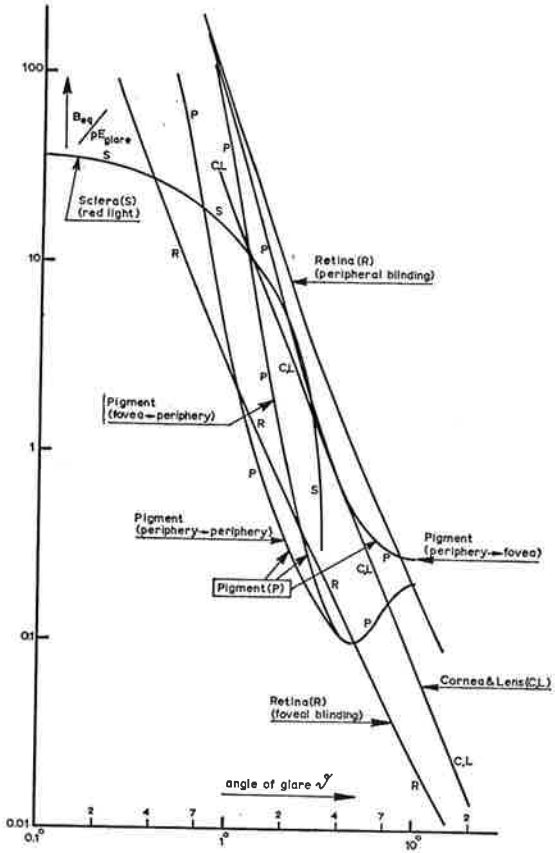

Fig. 8.4.1. The contribution of the various fundus components to the entoptic veil as a function of the glare angle. Revised version of Fig. 7.4.2.

angles of glare, it cannot compete with the other components, because its epicenter is too far away from the outer segments. For large angles, it is almost completely screened by the pigment sheet.

The cornea / lens curves, finally, are only based on mostly indirect experimental evidence. No theoretical concept forms its base.

Institute for Perception RVO-TNO
Soesterberg The Netherlands

October 1962

ON MECHANISMS OF GLARE

Summary

The subject of this thesis is the lowering of visibility in the presence of a glare source, shortly "glare". One disagrees, whether this phenomenon is only due to the masking action of entoptic straylight, or that there is a neural component as well (Chapter I). In the first part of our research, we tried to get clear about this controversy. We performed, for this purpose, comparative experiments about the masking of targets in the presence of a glare source on the one hand, and by adding an "ectoptic" luminous veil on the other. As a measure of the masking effect of the glare source, we used the "equivalent veiling brightness" (B_{eq}), i.e. that veil brightness, which just masks the same target. Obviously, B_{eq} depends on the angular distance to the glare source (the glare angle ϑ). Two things were found. B_{eq} proved to be proportional — with one exception, about which later on — to the glare intensity E (Chapter II) and independent of the target size (Chapter III). This is exactly what could be expected, if glare were a matter of straylight only. In that case, the equivalent veil simply represents the brightness of the entoptic veil. Should the masking influence be due to some neural inhibite activity, then B_{eq} would be of a formal nature only and its dependency on the glare intensity and the target size as described above would hardly be obvious. We concluded, that there is no evidence from our experiments for the existence of a neural glare component.

Therefore, we concentrated from then upon the problem, how the entoptic veil is constituted of contributions of the various scattering eye media. In some of the experimental conditions in Chapter II, the proportionality relation between B_{eq} and E is interrupted by an anomalous inflexion (Fig. 2.3.3). It could be explained in terms of the transition from rod to cone vision, in connection with the directional sensitivity of the cones. They are the cause, that straylight coming from the fundus is relatively suppressed at photopic brightness levels. Therefore, the magnitude of the inflexion informs us about the share of the fundus in entoptic straylight.

In fact, the fundus is a collective noun for the retina, the pigment layer, the choroid and the sclera together. The retinal share can be discerned from the other components by its dependence on the polarization of the glare light. With linearly polarized glare light, the scatter veil gets a winged structure ("Boehm brushes", Fig. 4.1.1) which is due to the retinal contribution. The difference in brightness between the dark and the bright wings was determined in various circumstances, and so we got an indication about the share of the retina (Chapter IV).

Another way to distinguish between the shares of the fundus and of the anterior eye media like cornea and lens, is to determine the change in the brightness of the entoptic veil, when the point of entry of the glare beam in the pupil is changed. The cornea / lens component is then gradually suppressed by the directional sensitivity of the cone receptors and shows the well known Stiles-Crawford effect. The fundus component keeps the same angle of incidence at the retina ($\approx 90°$) and remains unaffected. The actual lowering of the veil brightness appears to lie somewhere between these extremes and from its intermediate position, we could again derive a split up in a fundus and a cornea / lens share in the entoptic veil (Chapter V).

When a glare beam has a small cross section at its cornea transit, we can see the shadow of the iris on the retina as it is projected from the cornea as a scatter center. The brightness jump between this iris shadow and the pupil trans-illumination has been measured and gave us an insight in the contribution of the cornea to the entoptic veil (Chapter VI).

The results obtained in these experiments all point to a considerable share of the fundus in entoptic scattering and it seemed sensible therefore, to analyze theoretically the mechanism of fundus remission more detailed (Chapter VII). Successively, we passed in review: the receptive mechanism of the retina at these unusual angles of incidence and the scatter mechanisms of the retina, of the pigment coat behind it and of the sclerotic coat. We accounted for the influence of the foveal depression, of the transition from rod to cone vision, of the granularity of the pigment sheet and so on. As a result we came to a concept of the scatter mechanism of glare (Chapter VIII), summarized in a series of curves, indicating the course of the contribution of the various scattering eye media as a function of the angle of glare (Fig. 8.4.1).

The main conclusions of our research are:

a. Essentially, glare is a matter of light scattering in the eye.

b. The three principal sources of intra-ocular scatter are: the cornea, the crystalline lens and the fundus oculi. Roughly, their contributions have the same order of magnitude.

c. Glare is practically independent of the color of the incident light, and this can be understood fairly well theoretically.

d. In order to understand the contribution of the fundus, rough considerations are completely insufficient. A detailed research only, can lead to proper insight.

SAMENVATTING

Dit proefschrift heeft tot onderwerp de vermindering van het gezichtsvermogen in aanwezigheid van een verblindingsbron, kort gezegd „verblinding". Men verschilt van mening ten aanzien van de vraag of dit verschijnsel uitsluitend te wijten is aan verstrooiing van licht in het oog, of dat daarbij nog een nerveus verschijnsel komt (Hoofdstuk I). In het eerste deel van ons onderzoek trachtten wij een antwoord te geven op deze strijdvraag. We onderzochten de maskering van bepaalde toetsobjekten in aanwezigheid van een verblindingsbron én door een kunstmatig lichtwaas van buiten het oog. Maat voor het maskerend effekt van de verblindingsbron was de „equivalente" waashelderheid" — dat is de helderheid van het vergelijkingswaas dat hetzelfde toetsobjekt maskeert. Het zal duidelijk zijn, dat deze equivalente helderheid afneemt naarmate men verder weg kijkt van de verblindingsbron.

Onze bevindingen waren tweeërlei: de equivalente waashelderheid bleek in grote trekken evenredig te stijgen met de verblindingssterkte en zij bleek onafhankelijk te zijn van de grootte van de gekozen toetsobjekten (Hoofdstuk II en III). Dit is precies wat men zou moeten verwachten als de verblinding slechts een kwestie zou zijn van strooilicht. Dan stelt de equivalente helderheid eenvoudig de helderheid van het oogwaas voor. Zou de maskering het gevolg zijn van een nerveus onderdrukkingsproces — waarbij dus de zenuwbedrading over het verdere gezichtsveld in min of meerdere mate geblokkeerd zou worden — dan zou de equivalente waashelderheid slechts een formeel beschrijvend karakter dragen en zou een evenredigheid met de verblindingssterkte allerminst voor de hand liggen. Uit deze proeven is dan ook het bestaan van een nerveuze verblinding beslist niet komen vast te staan.

Eenmaal zover gekomen, richtten wij ons op de vraag, hoe dat oogwaas opgebouwd is uit bijdragen van de verscheidene oogmedia. Eén aanwijzing konden wij reeds putten uit het feit dat in sommige meetomstandigheden de evenredigheid tussen de waashelderheid en de verblindingssterkte onderbroken werd door een eigenaardige knik (Figuur 2.3.3). Deze knik kon worden verklaard uit een kombinatie van twee bekende verschijnselen: de geleidelijke verandering in de

wijze van zien met toenemende helderheid, in de schemer met de staafjes-receptoren, in helder licht met de kegeltjes; én de sterk naar de pupil gerichte lichtontvankelijkheid van de laatste. Hierdoor wordt men licht, dat aan de oogbodem wordt verstrooid, verhoudingsgewijs minder gewaar wanneer het lichtniveau stijgt. De grootte van de knik zegt ons daarom iets over de bijdrage van de oogbodem tot het oogwaas.

In feite is de uitdrukking „oogbodem" een verzamelnaam voor netvlies, pigmentlaag, vaatvlies en oogrok tezamen (Figuur 7.3.1). De bijdrage van het netvlies onderscheidt zich van die van de andere lagen door zijn afhankelijkheid van het trillingsvlak van het verblindende licht. Bij een in natuurlijk licht stralende verblindingsbron — waarbij dit vlak van moment tot moment wisselt — vertoont het oogwaas nauwelijks een struktuur. Maar is het verblindingslicht gepolarizeerd, dan krijgt het oogwaas een schoofstruktuur („Boehm-bundels", Figuur 4.1.1) die dus veroorzaakt wordt door de netvliesbijdrage. Het helderheidsverschil tussen de donkere en de lichte partijen werd bepaald in een aantal meetomstandigheden en hieruit verkregen wij aanwijzingen omtrent de bijdrage van het netvlies tot het oogwaas (Hoofdstuk IV).

Een andere manier om het strooilicht van de oogbodem te onderscheiden van dat van meer voor in het oog gelegen strooicentra (het hoornvlies, de ooglens; zie de foto op de frontpagina) is als volgt. Men bepaalt de verandering in de helderheid van het oogwaas als het verblindend licht het oog via verschillende plaatsen van de pupil binnentreedt. De reeds genoemde gerichtheid van de lichtontvankelijkheid van de netvlies-receptoren — wij beperken ons nu even tot de daglichtzin — maakt dat het strooilicht van hoornvlies en lens verminderd werkzaam is als de verblindende bundel via de pupilrand in plaats van via het centrum intreedt. Het strooilicht van de oogbodem daarentegen blijft scherend invallen en dus onveranderd werkzaam. De mate waarin de helderheid van het oogwaas de daling van de lichtontvankelijkheid van de receptoren volgt, geeft ons derhalve een indruk van de verhouding der bijdragen van hoornvlies en lens enerzijds en van de oogbodem anderzijds (Hoofdstuk V).

Als de verblindingsbundel nauw is, waar deze het hoornvlies passeert, dan zien we een schaduw zich aftekenen op het netvlies, die afkomstig blijkt van het regenboogvlies. De pupil wordt als het ware „doorgelicht" door het van het hoornvlies afkomstige strooilicht. De helderheidssprong tussen schaduw en doorlichtingsbeeld werd ge-

meten en wij kregen op deze wijze een inzicht in de bijdrage van de hoornvliesverstrooiing tot het oogwaas (Hoofdstuk VI).

Alle resultaten, verkregen uit de genoemde proeven, wijzen op een aanmerkelijk aandeel van de oogbodem tot het oogwaas — veel meer dan gewoonlijk wordt aangenomen.

Wij wijdden daarom enige nadere beschouwingen aan de wijze waarop de lichtverstrooiing aan de oogbodem tot stand komt (Hoofdstuk VII). Achtereenvolgens lieten wij de revue passeren: de reaktie van de receptoren op strijklicht en de verstrooiende eigenschappen van het netvlies, de pigmentlaag en de oogrok. Wij brachten de indeuking van het netvlies op de plaats van scherp zien in rekening, de overgang van schemerzin op daglichtzin, de korrelstruktuur van de pigmentlaag enz.

Als uiteindelijk resultaat kwamen wij tot een bepaalde opsplitsing van het oogwaas in haar samenstellende delen (Hoofdstuk VIII). Deze opsplitsing is samenvattend weergegeven in een aantal krommen, voorstellende het verloop van de bijdragen van de diverse oogdelen met de afstand tot de verblindingsbron (Figuur 8.4.1).

De voornaamste konklusies uit ons onderzoek zijn:

a. Verblinding is in wezen een kwestie van lichtverstrooiing in het oog.
b. De drie voornaamste bronnen van lichtverstrooiing in het oog zijn: het hoornvlies, de ooglens en de oogbodem. Ruwweg gezegd zijn hun bijdragen van dezelfde orde van grootte.
c. De verblinding is praktisch onafhankelijk van de kleur van het invallende licht, en dit kan theoretisch zeer wel worden begrepen.
d. Om de bijdrage van de oogbodem te begrijpen zijn globale beschouwingen ten enenmale ontoereikend. Slechts een zeer gedetailleerd onderzoek kan tot een redelijk inzicht voeren.

REFERENCES

The figures behind each reference indicate the sections of citation

M. J. Allen and *J. J. Vos:* in preparation 8.3

R. Barer: Refractometry and interferometry of living cells. J. Opt. Soc. Am. *47,* 545, 1957 7.3

W. Bargmann: Histologie und Mikroskopische Anatomie des Menschen, II, 4° Auflage. Georg Thieme Verlag, Stuttgart 1962 7.3

H. B. Barlow: Summation and inhibition in the frogs retina. J. Physiol. *119,* 69, 1953 1.2

W. Benary: Beobachtungen zu einem Experiment über Helligkeitskontrast. Psych. Forsch. *5,* 131, 1921 1.2

G. Boehm: Ueber ein neues entoptisches Phänomen im polarisierten Licht. Acta Ophth. *18,* 143, 1940 4.1,3

A. Borschke: Untersuchungen über die Herabsetzung der Sehschärfe durch Blendung. Zs. Psych. Phys. Sinnesorg. *34,* 1, 1904 7.9,10

M. A. Bouman: Peripheral contrastthresholds of the human eye. J. Opt. Soc. Am. *40,* 825, 1950 2.2

M. A. Bouman: Glare: "Actio in distans" via the retina or pure contrast phenomenon? Rep. Inst. f. Perc. 1953 - 14 3.1,3

M. A. Bouman: History and present status of quantum theory in vision. In "Sensory Communication", W. Rosenblith Ed., John Wiley & Sons, London/MIT Press, Boston 1960 3.1

M. A. Bouman: Quantumbiologie des Auges. Studium Generale *13,* 491, 1960 3.1

R. M. Boynton, W. R. Bush, and *J. M. Enoch:* Rapid changes in foveal sensitivity from direct and indirect stimuli. J. Opt. Soc. Am. *44,* 56, 1954 1.2

R. M. Boynton and *F. J. J. Clarke:* Sources of entoptic scatter in the human eye (abstract). J. Opt. Soc. Am. *52,* 1326, 1962 6.3

R. M. Boynton, J. M. Enoch and *W. R. Bush:* Physical measures of stray-light in excised eyes. J. Opt. Soc. Am. *44,* 879, 1954 1.2/6.1/8.2

G. S. Brindley and *E. N. Willmer:* The reflexion of light from the macular and peripheral fundus oculi in man. J. Physiol. *116,* 350, 1952 7.5,6,9/8.3

F. W. Campbell and *M. Alpern:* The pupillomotor spectral sensitivity curve and the color of the fundus. J. Opt. Soc. Am. *52,* 1084, 1962 7.5/8.3

P. W. Cobb: The influence of illumination of the eye on visual acuity. Am. J. Physiol. *29,* 76, 1911 2.1

P. W. Cobb and *L. R. Geissler:* The effect on foveal vision of bright surroundings. Psych. Rev. *20,* 425, 1913 1.2

D. W. DeMott: Direct measures of the retinal image. J. Opt. Soc. Am. *49,* 571, 1959 8.2,3

D. W. DeMott and *R. M. Boynton:* Sources of entoptic straylight. J. Opt. Soc. Am. *48,* 120, 1958 6.1,3/8.2,3

E. J. Denton: Light absorption by the intact retina. "Visual problems of colour", page 175, London 1957 7.2

A. Fiorentini and *A. M. Ercoles:* Vision of oscillating non-uniform fields. Optica Acta *4,* 150, 1957 1.2

F. Flamant: Etude de la répartition de lumière dans l'image rétinienne d'une fente. Rev. Opt. *34,* 433, 1955 8.2

F. Flamant and *W. S. Stiles:* The directional and spectral sensitivities of the retinal rods to adapting fields of different wavelength. J. Physiol. *107,* 187, 1948 2.4/8.3

G. A. Fry: A re-evaluation of the scatter theory of glare. Ill. Eng. *49,* 98, 1954 1.2/8.4

G. A. Fry and *M. Alpern:* The effect on foveal vision produced by a spot on the sclera near the margin of the retina. J. Opt. Soc. Am. *43,* 187, 1953 1.2

G. A. Fry and *M. Alpern:* Effect of a peripheral glare source upon the apparent brightness of an object. J. Opt. Soc. Am. *43,* 189, 1953 1.2

W. J. Geeraets, R. C. Williams, G. Chan, W. T. Ham, and *F. M. Schmidt:* The loss of light energy in retina and choroid. A.M.A. Arch. Ophth. *64,* 606, 1960 7.5

W. Goethe: Zur Farbenlehre I, Ch. 8. Tübingen 1810 1.2

H. Helmholtz: Ueber Herrn Brewsters Analyse des Sonnenlichtes. Ann. Physik und Chemie *86,* 501, 1852 1.2/2.3

L. L. Holladay: The fundamentals of glare and visibility. J. Opt. Soc. Am. *12,* 492, 1926 1.2/2.1,3

L. L. Holladay: Action of a lightsource in the field of view in lowering visibility. J. Opt. Soc. Am. *14,* 1, 1927 1.2/2.1,3

A. Ivanoff: Contribution à l'étude de la composante inhibitive de l'éblouissement. Rev. Opt. *26,* 479, 1947 2.4

H. E. Ives: Studies in the photometry of lights of different colours III. Phil. Mag. 24^6, 744, 1912 1.2

V. E. Kinsey: Spectral transmission of the eye to ultraviolet radiations. A.M.A. Arch. Ophth. *39,* 508, 1948 7.5

J. Krauskopf: Light distribution in human retina images. J. Opt. Soc. Am. *52,* 1040, 1962 8.2

S. W. Kuffler: Discharge patterns and functional organization of mammalian retina. J. Neurophysiol. *16,* 37, 1953 1.2

Y. le Grand: Sur deux propriétés des sources de lumière polarisée. C.R. Ac. Sc. *202,* 939, 1936 4.1

Y. le Grand: Diffusion de la lumière dans l'oeil. Rev. Opt. *16,* 201 and 241, 1937 1.2/2.1,3,4/4.2/7.9

Y. le Grand: Optique physiologique II. Ch. 16. Ed. Rev. Opt. Paris 1948 7.6

Y. le Grand: Optique physiologique III, page 164. Ed. Rev. Opt. Paris 1956 4.1

E. Ludvigh and *E. F. MacCarthy:* Absorption of visible light by the refractive media of the human eye. A.M.A. Arch. Ophth. *20,* 37, 1938 7.5

E. Mach: Ueber die Wirkung der räumlichen Vertheilung des Lichtreizes auf der Netzhaut. Sitz. Ber. Wien Akad. Wiss. *52/2,* 303, 1865 1.2

K. Motokawa: Field of retinal induction and optical illusions. J. Neurophysiol. *13,* 413, 1950 1.2

B. O'Brien: Vision and resolution in the central retina. J. Opt. Soc. Am. *41,* 882, 1951 7.2

D. G. Pitts: Transmission of the visible spectrum through the ocular media. Am. J. Optom. *30,* 209, 1959 7.5

G. I. Pokrowski: Ueber die Lichterstreuung im Auge. Zs. Physik *35,* 776, 1926 7.9

S. L. Polyak: The retina. Univ. Chicago Press 1941 7.3,4,6

J. Purkinje: Beobachtungen und Versuche zur Physiologie der Sinnesorgane I, Ch. 11 and 12, 1823 1.2

C. Roggenbau and *A. Wetthauer:* Ueber die Durchlässigkeit der brechenden Augenmedien für langwelliges Licht nach Untersuchungen am Rindsauge. Kl. Monatsbl. Augenhlk. *79,* 456, 1927 7.5

J. F. Schouten: Zur Analyse der Blendung. Proc. Kon. Akad. Wetensch. Amsterdam *37,* 506, 1934 1.2

J. F. Schouten: Visuele metingen van adaptatie. Thesis Utrecht 1937 1.2

J. F. Schouten and *L. S. Ornstein:* Measurements on direct and indirect adaptation by means of a binocular method. J. Opt. Soc. Am. *29,* 168, 1939 1.2

W. S. Stiles: The effect of glare on the brightness difference threshold. Proc. Roy. Soc. *104B,* 322, 1929 2.1,3

W. S. Stiles: The scattering theory of the effect of glare on the brightness difference threshold. Proc. Roy. Soc. *105B,* 131, 1930 1.2/8.4

W. S. Stiles and *B. H. Crawford:* The luminous efficiency of rays entering the eye at different points. Proc. Roy. Soc. *112B,* 428, 1933 5.1

W. S. Stiles and *B. H. Crawford:* The liminal brightness increment for white light for different conditions of the foveal and parafoveal retina. Proc. Roy. Soc. *116B,* 55, 1935 1.2

W. S. Stiles and *B. H. Crawford:* The effect of a glaring lightsource on extrafoveal vision. Proc. Roy. Soc. *122B,* 255, 1937 1.2/2.2,3

H. C. Van de Hulst: Light scattering by small particles. John Wiley & Sons, New York / Chapman & Hall, London 7.3,5

G. Van den Brink: Retinal summation and the visibility of moving objects. Thesis Utrecht 1957 1.2/3.2

G. Van den Brink and *M. A. Bouman:* Variation of integrative actions in the retinal system: an adaptational phenomenon. J. Opt. Soc. Am. *44,* 616, 1954 1.2/3.2

A. Vogt: Die Nervenfaserzeichnung der menschlichen Netzhaut im rotfreien Licht. Kl. Monatsbl. Augenhlk. *66,* 718, 1921 7.5

J. J. Vos and *M. A. Bouman:* Disability glare: theory and practice. Proc. CIE, Brussels 1959, page 298 2.3

J. J. Vos and *P. L. Walraven:* The Stiles-Crawford effect, a survey. Atti Fond. G. Ronchi *17,* 302, 1962 8.3

G. Wald: Human vision and the spectrum. Science *101,* 653, 1945 2.4

P. L. Walraven: On the mechanism of colour vision. Thesis Utrecht 1962 7.2

P. L. Walraven and *M. A. Bouman:* Relation between the directional sensitivity and the spectral response curves in human cone vision. J. Opt. Soc. Am. *50,* 780, 1960 7.2

G. Westheimer and *F. W. Campbell:* Light distribution in the image formed by the living human eye. J. Opt. Soc. Am. *52,* 1040, 1962 8.2

H. Wiesinger, F. H. Schmidt, R. C. Williams, C. O. Tiller, R. S. Ruffin, Dupont Guerry and *W. T. Ham jr.:* The transmission of light through the ocular media of the rabbit eye. Am. J. Ophth. *42,* 907, 1956 7.5

CONTENTS